May 24, 2013

The Honorable Fred Upton
Chairman
Energy and Commerce Committee
U.S. House of Representatives
2125 Rayburn House Office Building
Washington, D.C. 20515

The Honorable Henry A. Waxman
Ranking Member
Energy and Commerce Committee
U.S. House of Representatives
2322A Rayburn House Office Building
Washington, D.C. 20515

via email at: rfs@mail.house.gov

Dear Chairman Upton and Ranking Member Waxman:

Urban Air Initiative Inc. (UAI) respectfully submits its responses to the U.S. House of Representatives Committee on Energy and Commerce's White Paper Series on the Renewable Fuel Standard Questions for Stakeholder Comment. We are submitting our responses to Paper 3 released on May 9, 2013: Greenhouse Gas Emissions and Other Environmental Impacts.

UAI serves as an educational resource on urban air pollution and health problems caused by toxic emissions from motor vehicles. Supporters of UAI include alternative fuels producers, elected officials, medical experts, and anyone concerned about the harmful health effects caused by poor quality gasoline.

Please contact me at 316-927-4230 or via email at UrbanAirInitiative@gmail.com if you have questions.

Thank you for the opportunity to respond.

Sincerely,

Gregory P. Krissek, Director

Energy and Commerce Committee, RENEWABLE FUEL STANDARD ASSESSMENT WHITE PAPER, [Blend Wall/Fuel Compatibility Issues], Questions for Stakeholder Comment

> *1. Is the RFS reducing greenhouse gas emissions below that of baseline petroleum-derived fuels? Is the RFS incentivizing the development of a new generation of lower greenhouse gas emitting fuels?*

Urban Air Initiative responds to these two questions with an emphatic "yes." Contrary to what ethanol's detractors have claimed, even first-generation ethanol has a much smaller carbon footprint than baseline petroleum-derived fuels. In addition, ethanol's carbon benefits will grow substantially as its next-generation technology improvements are compared to the next generation of tar sands, oil shale, and fracking technologies.

The link referenced below is a recent essay published in the Physicians for Social Responsibility newsletter[1] which makes two important arguments: 1) an acre of corn, even after the starch portion of the grain is converted to nearly 500 gallons of "Clean Octane" ethanol,[2] yields the same amount of animal protein as does an acre of soybeans; and 2) an acre of corn—which is a highly efficient C4 crop compared to less efficient C3 crops—is a major carbon sink, rather than a carbon source, and makes the soil more fertile, more resistant to drought, and a more efficient user of water and nutrients. http://www.psr.org/environment-and-health/environmental-health-policy-institute/responses/corn-based-ethanol.html

Additional support for corn's role as a major carbon sink and contributor to increased soil organic matter (SOM) comes from recent USDA multi-year studies which were conducted and peer-reviewed by credible academic institutions. (**Attachment A** contains a spreadsheet listing the various studies and their findings. The Soil Organic Carbon sequestration data was assembled by Ron Alverson, Corn Producer, Chairman of Lake Area Corn Processors LLC, and President of the American Coalition for Ethanol).

As illustrated by the data, corn acres using minimum and no-till cultivation practices—which are used on more than 70% of U.S. corn acreage and increasing rapidly—have been shown to rebuild SOM--and sequester carbon--even better than switch grass, which has been highly touted as a sustainable feedstock for cellulosic ethanol production. Unfortunately, EPA and CARB modeling has thus far neglected to consider the deep root structure benefits of corn, and thus under-predicts corn's carbon sequestration benefits by 60–100%.

---

[1] Authored by Lt. Col. William C. Holmberg (USMC, ret.), American Council on Renewable Energy (ACORE)

[2] It may be useful to define two terms we use throughout the rest of this discussion. UAI uses the term "Clean Octane" to describe octane-boosting components (such as ethanol) that do not include carcinogenic aromatic compounds derived from crude oil. Conversely, we use the term "Dirty Octane" to describe the octane-boosting compounds known as aromatics, which refiners synthesize from crude oil, and which are the most toxic, carbon intensive, and expensive portion of gasoline. In the U.S., an average gallon of gasoline contains approximately 20–25% aromatics.

2. Could EPA's methodology for calculating lifecycle greenhouse gas emissions be improved, including its treatment of indirect land use changes? If so, how?

Yes. See the response to Question 1 above. We believe that EPA should conduct a thorough reassessment of the assumptions that were used five or more years ago concerning shifts in land use patterns and crop productivity trends. Most importantly, we urge the EPA to incorporate the new science that proves corn's ability to sequester carbon and restore SOM and vitality.

3. Is the definition of renewable biomass adequate to protect against unintended environmental consequences? If not, how should it be modified?

Urban Air Initiative does not have additional information to respond to this question.

4. What are the non-greenhouse gas impacts of the RFS on the environment relative to a comparable volume of petroleum-derived fuels? Is there evidence of a need for air quality regulations to mitigate any adverse impacts of the RFS?

UAI respectfully objects to the Committee's use of the word "mitigate" in question 4: "…to mitigate any adverse impacts of the RFS." We believe use of the word 'mitigate' in this context suggests that the Committee has already pre-determined that the increased use of ethanol is worse for the environment, "relative to a comparable volume of petroleum-derived fuels."

Last year, when EPA denied the petition to waive the RFS, the agency explained how petroleum refiners are taking advantage of ethanol's excellent octane properties to produce finished motor gasoline at the terminal, and reduce carcinogenic gasoline aromatics in the process.[3] EPA noted that "over the past 10 years, the economics of blending ethanol into gasoline have been such that many refiners have transitioned from producing primarily finished gasoline to producing primarily blendstocks for oxygenate blending (BOBs) which require the addition of ethanol in order to meet the specifications of finished gasoline." Later, EPA asserted that "Morgan Stanley argues that there would be significant impediments from moving away from ethanol because it is widely available and is the least expensive source of octane/oxygenates for most refineries." The good news is that the nationwide use of E10 as an octane booster has established a solid foundation for advancing to the next level as an octane-boosting transportation fuel. It is imperative to consider splash-blending higher volumes of ethanol in addition to the E10 base fuel to produce high quality performance E30+ blends to accommodate for the advanced engine technologies that will soon be dominating the U.S. light duty vehicle (LDV) fleet.

Upon request, Urban Air Initiative would be pleased to submit various peer-reviewed auto industry and health effects studies that have shown how higher levels of ethanol use—such as E30 blends (30% ethanol)—can substantially reduce the most potent pollutants. These criteria pollutants include NOx and fine and ultrafine particulate matter and the highly carcinogenic toxics that coat them (e.g., the polycyclic aromatic hydrocarbons, PAHs, which are hazardous air pollutants ["air toxics"]). Numerous experts have confirmed that E30 blends reduce particulate matter (PM), particulate number (PN), and black carbon (a climate change agent many times

---

[3] "Notice of Decision Regarding Requests for a Waiver of the Renewable Fuels Standard", EPA, Federal Register/Vol.77, No. 228, November 27, 2012, 70759 – 70760.

more powerful than carbon dioxide) by 45–80% or more in both direct injection and port fuel injection engines. Other studies warn that unless EPA improves gasoline composition by reducing aromatic concentrations (which Congress directed it to do in the 1990 Clean Air Act Amendments), particle-borne PAH emissions will increase as advanced engine technologies like direct injection (DI) dominate the light duty vehicle fleet in order to meet stricter fuel economy standards in coming years.

On May 16, 2013, the Wild Earth Guardians sued EPA for its failure to properly control urban PM2.5 levels in Salt Lake City, Utah, where more than 50% of the particulates originate from motor vehicles. Urban Air Initiative believes that EPA's failure to act on enforcing the control of urban PM2.5 levels is that its models substantially under-predict the secondary organic aerosol (SOA) formation that originates primarily from gasoline aromatics, something that EPA publicly admitted more than seven years ago.

The attached study titled, "Combustion efficiency and engine out emissions of a spark-ignition engine fueled with alcohol/gasoline blends," by M.A. Costagliola et al, is labeled as **Attachment B**. This study explains the relative toxicity of the PAHs compared to other air toxics such as acetaldehydes. EPA's draft Tier 3 rulemaking acknowledges that PAHs are potent MSATs, and that PAH emissions have been increasing in recent years due to increased gasoline use. In addition to their ubiquitous presence in urban air sheds, the increased deposition of PAHs in the nation's waterways is an increasingly serious problem. Inexplicably, however, EPA's models continue to exclude PAHs, even though these compounds are thousands of times more toxic than acetaldehydes.

5. *Has implementation of the RFS revealed any environmental challenges or benefits not fully anticipated in the statute?*

Urban Air Initiative does not have additional information to respond to this question.

6. *What is the optimal percentage of ethanol in gasoline?*

Increasingly, automakers such as Mercedes Benz are recommending the widespread use of E30 blends to provide Clean Octane for higher compression, more efficient, and cleaner burning engines of the future. [See May 3, 2013 *New York Times* article by Matt Wald, "Squeezing more out of ethanol".] http://www.nytimes.com/2013/05/05/automobiles/squeezing-more-from-ethanol.html

Many experts believe that the E30 blend range represents the "sweet spot" for ethanol's superior octane properties. Multiple performance studies conclude that E30 provides optimum octane boost, avoids most of the energy density penalties of E85, and ensures substantial reductions in a wide range of harmful emissions. As E30 blends become widely available, ethanol's inherent high-octane rating will allow automakers to optimize their engines by increasing compression ratios to levels not possible with standard gasoline blends, thereby avoiding any mileage loss due to ethanol's energy content.

The 2012 Costagliola et al study cited in Attachment B and the 2012 Maricq/Ford et al. study cited in **Attachment C** elaborate on the many performance and emissions benefits of E30.
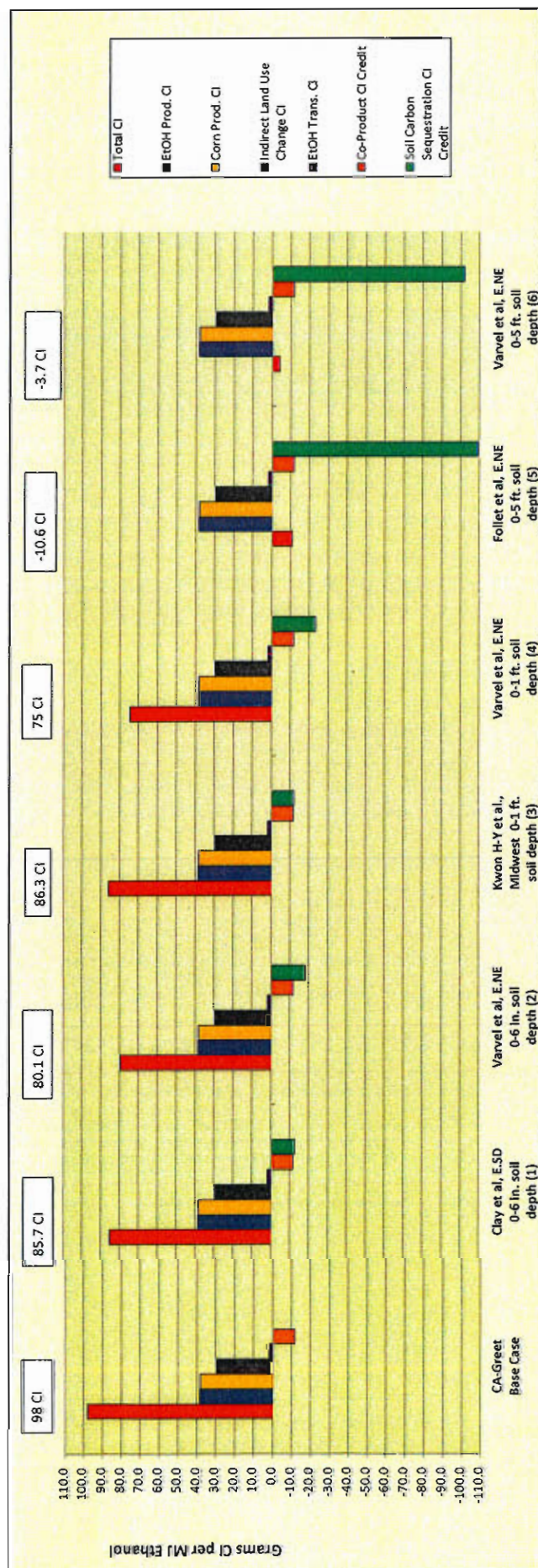
In addition, E30 blends would also save motorists at the fuel pump, since ethanol is an octane provider that costs much less than energy-intensive aromatics, which only get more expensive as crude oil costs increase.

7. *What are the best options for substantially further reducing greenhouse gas emissions from the transportation sector?*

As public comments submitted by UAI to both the Greenhouse Gas (GHG)–Corporate Average Fuel Economy (CAFE) and PM2.5 rulemaking dockets made clear, gasoline aromatics are not only the most toxic and expensive gasoline components, they are also the most carbon intensive. By replacing the "dirty octane" elements that are in aromatics with "clean octane" in E30+ blends, the U.S. transportation sector would achieve substantially more GHG emission reductions, and these carbon benefits would grow over time as the much more carbon intensive tar sands and oil shale crude feedstocks increase their market share. Coupled with the new science referred to in Question 1 that proves corn's substantial ability to sequester carbon, E30+ blends offer one of the most cost effective, commercially available, and environmentally safe ways to reduce gasoline's carbon footprint in the near- to mid-term.

The Effect of Soil Organic Carbon Sequestration Credits on Corn Ethanol Life Cycle CI (Carbon Intensity)

(A comparison of calculated credits from 6 recent midwest SOC sequestration studies, with the California GREET Model Base Case Carbon Intensity)

Chart legend:
- Total CI
- EtOH Prod. CI
- Corn Prod. CI
- Indirect Land Use Change CI
- EtOH Trans. CI
- Co-Product CI Credit
- Soil Carbon Sequestration CI Credit

Y-axis: Grams CI per MJ Ethanol (110.0 to -110.0)

CA-Greet Base Case	Clay et al, E.SD 0-6 in. soil depth (1)	Varvel et al, E.NE 0-6 in. soil depth (2)	Kwon H-Y et al., Midwest 0-1 ft. soil depth (3)	Varvel et al, E.NE 0-1 ft. soil depth (4)	Follet et al, E.NE 0-5 ft. soil depth (5)	Varvel et al, E.NE 0-5 ft. soil depth (6)
98 CI	85.7 CI	80.1 CI	86.3 CI	75 CI	-10.6 CI	-3.7 CI

[1] https://www.agronomy.org/publications/ajl/abstracts/104/3/763

[2] http://digitalcommons.unl.edu/cgi/viewcontent.cgi?article=1224&context=usdaarsfacpub&sei-
redir=1&referer=http%3A%2F%2Fwww.google.com%2Furl%3Fsa%3Dt%26rct%3Dj%26q%3Dsoil%2520carbon%2520carbon%2520levels%2520in%2520irrigated%2520western%2520corn%2520belt%2520rotations%2520corn%2520belt%2520rotations%26source%3Dweb%26cd%3D1%26sql%3D2%26ve
d%3D0CDQQFjAA%26url%3Dhttp%253A%252F%252Fdigitalcommons.unl.edu%252F2Fcgi%252Fviewcontent.cgi%253Farticle%253D1224%2526context%253Dusdaarsfacpub%26ei%3DSVSrUcTaH-
eByqHF14GQAg%26usg%3DAFQjCNGZtydWf7_gWzem0MO39gOayo_dUw#search=%22soil%20carbon%20levels%20irrigated%20western%20corn%20belt%20rotations%22

[3] http://www.sciencedirect.com/science/article/pii/S0961953413000950

[4] https://www.soils.org/publications/sssaj/abstracts/74/3/915?access=0&view=pdf

[5] http://link.springer.com/article/10.1007%2Fs12155-012-9198-y#page-1

[6] http://digitalcommons.unl.edu/agronomyfacpub/591/

Chart notes of explanation:

Starting on the left side of the chart, the first set of bars are the corn EtOH life cycle emissions calculated using the default values from the California GREET model. Note that total Carbon Intensity is 98. The 98 is a total of the next 6 bars in the group. - 1) emissions from EtOH production at the plants, 2) emissions from corn production on farms, 3) emissions from Indirect Land Use Change, 4) emissions from EtOH transportation and distribution, 5) emissions credits for co-products, and 6) emission credits for soil carbon sequestration. Each succeeding set of bars is described by the footnote and shows the same exact emissions for ethanol production, corn production, ILUC, EtOH transportation and distribution, co-product credits, and the variable (soil carbon sequestration credits) found in that study. So, the only variable is the credit for soil carbon sequestration. I thought it would be helpful to show where all the sources of emissions are from on the chart, but perhaps that adds unnecessary information? Anyway, you will undoubtedly notice that studies that only quantified soil carbon sequestration in topsoils, reduce CI significantly (10-15%) and those that tested full soil profiles resulted in dramatic reductions in CI.

Ron Alverson

Corn Yields and No-Tillage Affects Carbon Sequestration and Carbon Footprints

David E. Clay,* Jiyul Chang, Sharon A. Clay, James Stone, Ronald H. Gelderman,

Gregg C. Carlson, Kurtis Reitsma, Marcus Jones, Larry Janssen, and Thomas Schumacher

Table 4. The influence of sampling region and the short-term sequestered C rates on partial C footprints for the 2004 to 2007 and 2008 to 2010 time periods - from South Dakota State University soil test lab database - 0-6 inch soil sampling depth

S.D. Region	2004 to 2007 Sequestered Carbon kg SOC/ha/yr	2004 to 2007 Partial Carbon Footprint g CO2eq/Mj	2008 to 2010 Sequestered Carbon kg SOC/ha/yr	2008 to 2010 Partial Carbon Footprint g CO2eq/Mj		2004 to 2007 Estimated Ethanol Value Increase @ $38/Mg Carbon Credit $/gallon	2008 to 2010 Estimated Ethanol Value Increase @ $38/Mg Carbon Credit $/gallon
North Central	229	-14.9	412	-19.6	-16.9143	$ 0.045	$ 0.060
Central	69	-5.1	329	-14.8	-9.25714	$ 0.016	$ 0.045
Northeast	182	-8.9	231	-12.0	-10.2057	$ 0.027	$ 0.036
East-central	125	-6.3	264	-11.4	-8.49143	$ 0.019	$ 0.035
Southeast	266	-14.9	454	-19.2	-16.7429	$ 0.045	$ 0.058
					-12.3223		

Carbon footprint values reported as negative numbers in this study to represent a CI reduction

Table 4 from page 759
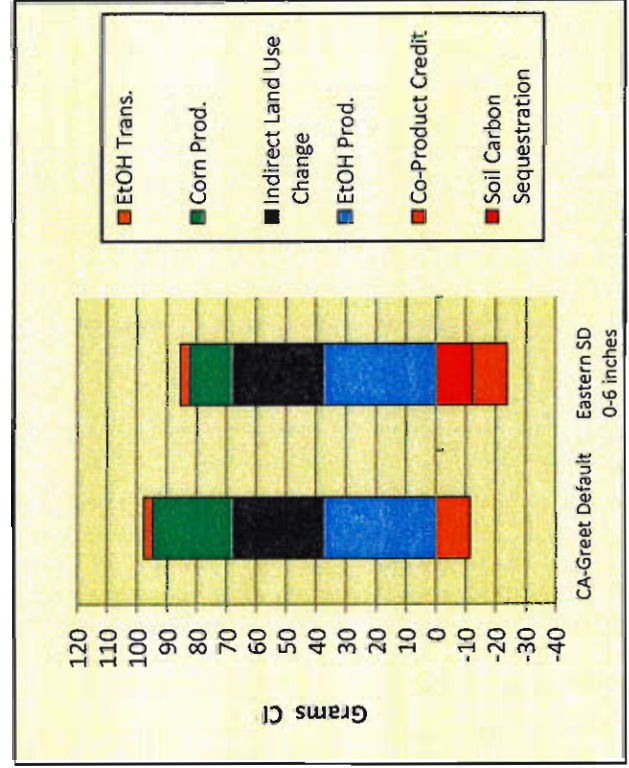
Soil Organic Carbon Levels in Irrigated Western Corn Belt Rotations

G.E. Varvel and W.W. Wilhelm

Published in Agronomy Journal, 100:1180–1184 (2008).

Change in SOC (1991-2005) in the 0-15 cm topsoil

(@ 200 kg/ha Nitrogen application rate (corn))

Tillage system = Disk 2X

Site had been in irrigated continuous corn for more than 10 yrs prior

	14 Year increase in SOC	Annual increase in SOC	Annual increase in SOC	1991 Organic Matter	2008 Organic Matter
	Mg/ha	Mg/ha	lb/ac	%	%
Continuous Corn	6	0.429	382	1.54%	2.00%
Corn - Soy	3.5	0.250	223	1.54%	1.81%
Continuous Soy	1.8	0.129	115	1.54%	1.68%

Corn Ethanol Annual Carbon Intensity Reduction	Estimated Corn Ethanol Value Increase (@ $38/Mg)
gCO2eq/MJ	$/gal
17.9	$ 0.054
10.4	$ 0.032
5.4	$ 0.016

From figure 1 on page 1183

Modeling state-level soil carbon emission factors under various scenarios for direct land use change associated with United States biofuel feedstock production

Ho-Young Kwon, Steffen Mueller, Jennifer B. Dunn, Michelle M. Wander

Projected Soil C Emission Factors (Sequestration rates in Mg C ha yr in 0-30 cm soil depth)

Cropland conversion to corn for bioenergy production in 11 corn belt states

Figure 3. page 9

		Soil C Emission Factors Mg C ha yr	Soil C Emission Factors Lbs C ac yr	Corn Ethanol Annual Carbon Intensity Reduction gCO2eq/MJ	Estimated Corn Ethanol Value Increase (@ $38/Mg) $/gal
Baseline 2010 current conditions	No till Corn - 30% stover harvest	-0.25	-223	10.4	$ 0.032
	Reduced till corn - 30% stover harvest	-0.18	-161	7.5	$ 0.023
	Conventional till corn - 30% stover harvest	-0.1	-89	4.2	$ 0.013
	No till Corn - zero stover harvest	-0.36	-321	15.0	$ 0.046
	Reduced till corn - zero stover harvest	-0.28	-250	11.7	$ 0.036
	Conventional till corn - zero stover harvest	-0.25	-223	10.4	$ 0.032
Yield-up 2040 Future trendline yields	No till Corn - 30% stover harvest	-0.49	-437	20.5	$ 0.062
	Reduced till corn - 30% stover harvest	-0.4	-357	16.7	$ 0.051
	Conventional till corn - 30% stover harvest	-0.36	-321	15.0	$ 0.046
	No till Corn - zero stover harvest	-0.64	-571	26.7	$ 0.081
	Reduced till corn - zero stover harvest	-0.56	-500	23.4	$ 0.071
	Conventional till corn - zero stover harvest	-0.51	-455	21.3	$ 0.065
Decay-up (increased cultivation & fertilization)	No till Corn - 30% stover harvest	-0.16	-143	6.7	$ 0.020
	Reduced till corn - 30% stover harvest	-0.11	-98	4.6	$ 0.014
	Conventional till corn - 30% stover harvest	-0.04	-36	1.7	$ 0.005
	No till Corn - zero stover harvest	-0.28	-250	11.7	$ 0.036
	Reduced till corn - zero stover harvest	-0.21	-187	8.8	$ 0.027
	Conventional till corn - zero stover harvest	-0.14	-125	5.8	$ 0.018
Yield-up Decay-up	No till Corn - 30% stover harvest	-0.37	-330	15.5	$ 0.047
	Reduced till corn - 30% stover harvest	-0.28	-250	11.7	$ 0.036
	Conventional till corn - 30% stover harvest	-0.25	-223	10.4	$ 0.032
	No till Corn - zero stover harvest	-0.5	-446	20.9	$ 0.064
	Reduced till corn - zero stover harvest	-0.4	-357	16.7	$ 0.051
	Conventional till corn - zero stover harvest	-0.35	-312	14.6	$ 0.044

Negative factors indicate Soil C sequestration
Positive factors indicate Soil C emissions

Long-term Soil Organic Carbon as Affected by Tillage and Cropping System

G.E. Varvel, W.W. Wilhelm

Table 4. Change in soil organic C concentrations from 1989 to 2004 in the 0 to 7.5, 7.5 to 15, and the 15 to 30 cm depths as affected by five tillage treatments in plots in the first three replications planted to corn at the Rogers Memorial Farm near Lincoln, NE.

Continuous corn portion of study

| Tillage | Change in SOC (1989-2004) | | | Total Increase SOC | Annual Increase | Corn Ethanol Carbon Intensity Reduction | Estimated Ethanol Value Increase @ $38/Mg |
	0-7.5 cm	7.5-15 cm	15-30 cm	Lbs/Ac.	Lbs/Ac.	gCO2eq/Mj	$/gallon
	------- g C kg -------						
Chisel	2.24	1.24	1.3	6,080	405	19	$ 0.058
Disc	3.38	1.3	1.12	6,920	461	22	$ 0.066
Plow	0.33	0.47	1.43	3,660	244	11	$ 0.035
No-till	4.65	1.83	1.71	9,900	660	31	$ 0.094
Sub-till	3.17	1.39	2.91	10,380	692	32	$ 0.098

Table 4 on page 921

23

Soil Carbon Sequestration by Switchgrass and No-Till Maize grown for Bio Energy

Ronald F. Follett, Kenneth P. Vogel, Gary E. Varvel, Robert B. Mitchell, John Kimble

Published 4 May 2012 in BioEnergy Research ISSN 1939-1234, Volume 5, Number 4

9 Year study (1998-2007)

C sequestration in 0-150 cm soil profile

Study site has extremely variable soils including several sand lenses mixed throughout

Crop	SOC Sequestration 1998 - 2007 Mg C/ha	Annual SOC Sequestration Mg C/ha	Annual SOC Sequestration lbs/ac	Corn Ethanol Sequestration Credit (gCO2eq/Mj)	Estimated Ethanol Value Increase @ $38/Mg ($/gallon)
Switchgrass	18.0	2.0	1,785	84	$ 0.25
No-Till Maize	23.4	2.6	2,320	109	$ 0.33

From
Discussion
on page 873

No-Tillage increases soil profile Carbon and Nitrogen under long-term rainfed cropping systems

G.E. Varvel, W.W. Wilhelm

Table 3

Total SOC values as affected by tillage treatment and cropping system at the 0-15, 15-30, 30-60, 60-90, and 120-150-cm depths in 1999 at the Roger's Memorial Farm near Lincoln, NE.

Tillage	Depth (cm)					
	0-15	15-30	30-60	60-90	90-120	120-150
	Total SOC (Mg ha)					
Chisel	33.3	24.0	27.4	15.3	12.9	9.8
Disk	34.9	26.6	37.3	27.1	21.6	13.6
Plow	31.8	28.3	28.6	17.1	14.8	11.0
No-till	37.7	31.3	41.5	27.2	21.0	12.6
Ridge Till	36.3	30.0	38.2	24.6	18.8	12.6
Subtill	32.4	26.7	36.4	27.7	21.9	14.3
Cropping System						
CC	36.6	28.6	36.1	22.6	18.4	12.1
SB-C	34.1	28.0	35.6	23.6	18.6	12.1
CSB	32.5	26.8	33.0	23.3	18.5	12.7

Table 3 on Page 32

Table 5

Depth (cm)					Difference Mg/ha	% OM	Difference % OM	Difference Lbs/ac	Annual gCO2 eq/Mj Annual CI diff.	Estimated Corn Ethanol Value Increase (@$38/Mg) $/Gal
0-30	0-60	0-90	0-120	0-150						
57.3	84.7	100.0	112.9	122.7	0.0	2.01%	0.00%	0	-	-
61.5	98.8	125.9	147.5	161.1	38.4	2.64%	0.63%	8,975	115	$ 0.35
60.1	88.7	105.8	120.6	131.6	8.9	2.15%	0.15%	2,080	27	$ 0.08
69.0	110.5	137.7	158.7	171.3	48.6	2.80%	0.80%	11,359	145	$ 0.44
66.3	104.5	129.1	147.9	160.5	37.8	2.63%	0.62%	8,835	113	$ 0.34
59.1	95.5	123.2	145.1	159.4	36.7	2.61%	0.60%	8,578	110	$ 0.33
									102	0.30915
65.2	101.3	123.9	142.3	154.4	7.6	2.53%	0.21%	1,776	23	$ 0.07
62.1	97.7	121.3	139.9	152.0	5.2	2.49%	0.14%	1,215	16	$ 0.05
59.3	92.3	115.6	134.1	146.8	0.0	2.40%	0.00%	-	-	-

Table 5 on page 33

0.46%
2.85%

0
0
0

Combustion efficiency and engine out emissions of a S.I. engine fueled with alcohol/gasoline blends

M.A. Costagliola, L. De Simio, S. Iannaccone, M.V. Prati *

Istituto Motori, National Council of Research, viale Marconi, 8, 80125 Napoli, Italy

HIGHLIGHTS

▶ The effect of ethanol was studied in S.I. engine at standard pressure peak position.
▶ A slightly better global efficiency (~5%) was achieved with E85 compared to gasoline.
▶ Particle number emissions were reduced (~90%) with ethanol blends.
▶ A 50% reduction of benzene and 1,3-butadiene emissions was achieved with E85 blend.

ARTICLE INFO

ABSTRACT

In this experimental work, the influence of some bio-fuels on the spark-ignition engine combustion efficiency and engine-out emissions was investigated. A conventional 1.6 l port injection engine was tested over steady-states, with some bio-ethanol/gasoline blends (0, 10, 20, 30, and 85 vol% of ethanol in gasoline) and with a 10 vol% of n-butanol in gasoline. Study of combustion development was made through the heat release analysis of pressure cycles measured in combustion chamber. Regulated emissions, unregulated organics (Polycyclic Aromatic Hydrocarbons, carbonyl compounds and Volatile Organic Compounds) and particulate were measured. Particulate was characterized in terms of total particle number (PN) and size distribution between 7 nm up to 10 μm. The tests were carried out at stoichiometric conditions in closed loop and spark advance was optimized with a calibration tool software in order to have the same peak pressure position. By fueling the alcohol blends, the engine-out particulate emissions are strongly reduced compared to gasoline. The PN reduction percentage ranges between 60% and 90%. The benefits also concern some gaseous unregulated species very harmful for humans, such as benzene and benzo(a)pyrene (reduction of almost 50% and 70% respectively). The highest oxygen content of alcohol blends, instead, provides an increasing of the total carbonylic emissions.

1. Introduction

In recent years, the strong restrictions applied to emissions from road transport together with the scarce availability of conventional fuels responsible for a constant increasing of fuel prices have encouraged the research activity towards alternative fuels. An increasing use of bio-fuels for transport is emerging as an important policy strategy to replace petroleum fuels. The European Union (EU) was aimed at achieving a 5.75% target of biofuels by 2010 (calculated on the basis of energy content), set by the EU Directive 2009/28/EC on the promotion of the use of energy from renewable sources and adopted by most Member States in their national biofuel objectives. Bio-ethanol is a renewable energetic source, and therefore it can contribute to reduce green house gas emissions. The benefits are as much high as greater is the efficiency of ethanol global productive process, taking into account also land use competition with other human needs. Bioethanol can be produced from various kinds of biomass such as corn, sugarcane, sugar beet, cassava, and red seaweed. It is one of alternative fuels most employed because of its oxygen content which favors the further combustion of gasoline. Besides, gasoline blends well with ethanol, compared to diesel, resulting in lower sulfur and aromatics content, higher octane number, and higher vapor pressure compared to the base fuel. Recently, the attention towards n-butanol as alternative fuel is increasing due to its high affinity with gasoline. Moreover, n-butanol when blended with gasoline is characterized by a high stability: in presence of water, in fact, n-butanol/gasoline blends do not separate. The most negative aspect is toxicity to humans from excessive exposition to n-butanol.

The influence of alcohol/gasoline blends on spark ignition internal combustion engine performance and emission was largely

* Corresponding author. Tel.: +39 0817177210; fax: +39 0812396097.
  E-mail address: m.v.prati@im.cnr.it (M.V. Prati).

2   M.A. Costagliola et al./Applied Energy xxx (2012) xxx–xxx

investigated. Bibliographic data highlight a general reduction of engine out emissions [1,2]. Also a positive effect of alcohol content on thermal efficiency was noted, both on a single cylinder engine at the test bed [3] and on a vehicle on a chassis dynamometer [4]. In [5] a passenger car equipped with a SI engine showed on a chassis dynamometer a 6% efficiency increasing when 50% of isobutanol/gasoline blend was used at full admission. Instead with pure isobutanol efficiency was reduced by 9%. In [6] the authors have tested oxygenated blends up to 15% by volume in gasoline on a single cylinder motorcycle engine. They highlight benefit on HC and CO emission and increased thermal efficiency. Blending ethanol with gasoline was also found to permit a higher compression ratio without knock occurrence [7]. Oxygenated blends were tested also with new concept strategy like homogeneous charge compression ignition (HCCI) and dual-injection. In [8] the authors found a reduction of NOx emission in a HCCI engine at butanol volume percentage increasing due to a lower maximum in-cylinder temperature. In [9] a two cylinders diesel engine was modified to operate in a HCCI mode in one cylinder with pure ethanol. The other cylinder was retained in normal diesel mode to motor the second cylinder. The authors report a stable HCCI combustion with an air intake temperature of 120–150 °C until a bmep of 4.3 bar. Dual injection (port fuel and direct injection) was tested [10,11] on a single cylinder engine with the aim of emphasizing the cooling-effect of oxygenated fuel with heat of vaporization higher than gasoline. The fossil fuel is port fuel injected while the biofuels is direct injected. This reduces the charge temperature and in turn reduces NOx and knock tendency while increases efficiency. A review of ethanol/gasoline blends impact on internal combustion engine is given in [12]. Besides, few publications are available on the effects of these alternative fuels on harmful emissions such as fine particles and carcinogenic organic compounds. In [13] an increment of ethanol, formaldehyde and acetaldehyde was observed when fueling a S.I. engine with low blend ethanol gasoline blends (maximum E20) at relative low temperature (<900 K). A recent study confirm that the emission of acetaldehyde significantly increased using E3 as fuel at the exhaust of nine four-stroke motorcycle [14]. About particulate, results showed in [15] highlight a PM increment at the exhaust of a direct injection engine by increasing the ethanol content related to a lower mixture homogeneity. According [16] n-butanol addition can decrease particle number concentration emissions compared with that of gasoline. This study has the objective of characterizing the engine behavior with several gasoline/ethanol and butanol blends in terms of emissions and performance (mainly efficiency and combustion development). In particular, steady-state tests were carried out on a conventional port injection spark ignition engine 1.6 l displacement fueled with gasoline, E10, E20, E30, E85 and n-B10 (respectively 10%, 20%, 30%, 85% v/v of ethanol and 10% of normal butanol in gasoline). Comparative studies of combustion development of gasoline and gasoline/ethanol blends at different concentrations have been made through the analysis of pressure cycles measured in combustion chamber. Moreover regulated emissions and unregulated organic emissions (Polycyclic Aromatic Hydrocarbons – PAHs, carbonyl compounds and Volatile Organic Compounds – VOCs) were collected and analyzed. Particulate matter was characterized in terms of particle number (PN) emissions and size distribution by an ELPI (Electrical Low Pressure Impactor) sampling system.

2. Materials and methods

2.1. Engine

The engine used in the tests is a conventional 1.6 l spark ignition (volumetric compression ratio 10.5), timed port injection with a three-way catalyst at the exhaust. For the optimization of engine parameters and ECU (Electronic Control Unit) data storage, the Magneti Marelli HELIOS software was used. The engine was instrumented with a pressure transducer in the combustion chamber of cylinder nos. 3 and 29 thermocouples to monitor the temperature in significant points, such as intake and exhaust manifold, the seat between intake and exhaust valve, and the zone close to the spark plug.

The tests were carried out on a grid of 9 speed/load points, ranging from 1750 to 3000 rpm and from 20 to 80 Nm, besides idle condition. In Fig. 1 the nine experimental points carried out with an evident high repeatability in the mid/low engine speed/load operating area are shown.

2.2. Fuels

Six test fuels were used in this study. A commercial gasoline was used as base fuel for the preparation of all the blends. Bioethanol, obtained from grape pomace produced during traditional wine processing, was provided by I.M.A. srl (Trapani, Italy). Four bioethanol–gasoline splash blends were prepared with 10%, 20%, 30% and 85% ethanol by volume in gasoline, named as E10, E20 E30 and E85, respectively. Also a normal butanol/gasoline blend 10% v/v (nB10) was tested for the higher affinity with gasoline characteristics. Selected fuel properties are shown in Table 1.

A not negligible oxygen content (1.5% by mass) in gasoline and a heat value of 42.7 MJ/kg were considered. Pure ethanol has lower A/F mass ratio and heat value, but energy content for mass unit
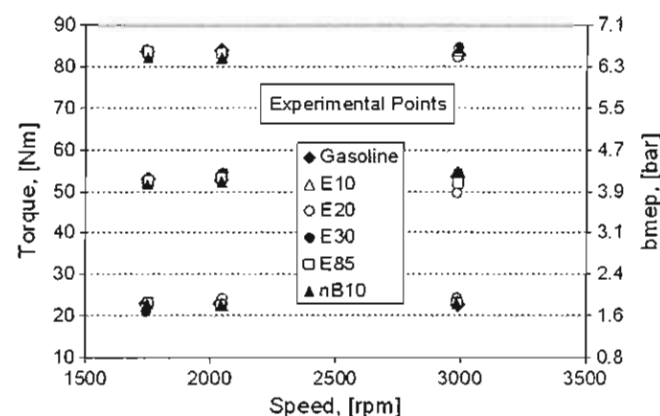

Fig. 1. Experimental points in the mid/low speed/torque area of the 1.6 l spark ignition engine fueled with gasoline and alcohol/gasoline blends.

Table 1
Main characteristics of the tested fuels.

FUEL	A/F (kg/kg)	H_i[a] (MJ/kg)	ρ (kg/m^3)	gCO_2/ MJ g/MJ	Cooling effect[b] (°C)	$H_{st,mix}$[c] (MJ/kg)	H_v[d] (kJ/kg)
Gasoline	14.3	42.7	750	73	24	2.78	349
nB10	14.0	42.0	756	72	26	2.80	358
E10	13.8	41.0	754	73	30	2.78	409
E20	13.2	39.4	757	73	35	2.77	468
E30	12.7	37.8	761	73	42	2.76	527
E85	9.8	29.2	780	71	86	2.71	840
Butanol	11.2	36.1	810	66	38	2.96	430
Ethanol	9.0	26.9	785	71	102	2.69	923

[a] Heat value.
[b] Estimated considering air as an ideal gas mixture with specific heat at constant pressure of 1 kJ/kg °C.
[c] Heat content of stoichiometric mixture.
[d] Heat of vaporization.

3

Table 2
List of gaseous unregulated pollutants.

Compound	Group	IARC class[a]	Compound	Group	IARC class[a]
Naphthalene	PAHs	2B	o-Toluoladehyde	Carbonyl.	n.a.
Acenaphtilene	PAHs	3	m-Toluoladehyde	Carbonyl.	n.a.
Acenaphtene	PAHs	3	p-Toluoladehyde	Carbonyl.	n.a.
Fluorene	PAHs	3	Hexaldehyde	Carbonyl.	n.a.
Phenanthrene	PAHs	3	2,5-Dimethylbenzaldehyde	Carbonyl.	n.a.
Anthracene	PAHs	3	Methane	VOC	n.a.
Fluoranthene	PAHs	3	Ethane	VOC	n.a.
Pyrene	PAHs	3	Ethylene	VOC	3
Benzo(a)anthracene	PAHs	2B	Propane	VOC	n.a.
Chrysene	PAHs	2B	Propylene	VOC	3
Benzo(b + k + j)fluoranthene	PAHs	2B	Acetylene	VOC	n.a.
Benzo(e)pyrene	PAHs	3	i-Butane	VOC	n.a.
Benzo(a)pyrene	PAHs	1	Propadiene	VOC	n.a.
Perilene	PAHs	3	n-Butane	VOC	n.a.
Indeno(1,2,3,c,d)pyrene	PAHs	2B	Trans-2-butene	VOC	n.a.
Dibenzo(a,h)anthracene	PAHs	2A	1-Butene	VOC	n.a.
Benzo(g,h,i)perylene	PAHs	3	i-Butene	VOC	n.a.
Dibenzo(a,e)pyrene	PAHs	3	Cis-2-butene	VOC	n.a.
Coronene	PAHs	3	2,2-Dimethylpropane	VOC	n.a.
Dibenzo(a,h)pyrene	PAHs	2B	2-Methylbutane	VOC	n.a.
Dibenzo(a,i)pyrene	PAHs	2B	Propine	VOC	n.a.
Dibenzo(a,l)pyrene	PAHs	2A	1,3-Butadiene	VOC	1
Formaldehyde	Carbonyl.	1	2,2-Dimethylbutane	VOC	n.a.
Acetaldehyde	Carbonyl.	2B	Butine	VOC	n.a.
Acrolein	Carbonyl.	3	2-Methylpentane	VOC	n.a.
Acetone	Carbonyl.	n.a.	3-Methylpentane	VOC	n.a.
Propionaldehyde	Carbonyl.	n.a.	Benzene	VOC	1
Crotonaldehyde	Carbonyl.	3	Toluene	VOC	3
Butyraldehyde	Carbonyl.	n.a.	Ethylbenzene	VOC	2B
Benzaldehyde	Carbonyl.	n.a.	m + p-Xylene	VOC	3
Isovaleraldehyde	Carbonyl.	n.a.	o-Xylene	VOC	3
Valeraldehyde	Carbonyl.	n.a.			

[a] Group 1 carcinogenic to humans; Group 2A probably carcinogenic to humans; Group 2B possibly carcinogenic to humans; and Group 3 not classifiable as to its carcinogenicity to humans.
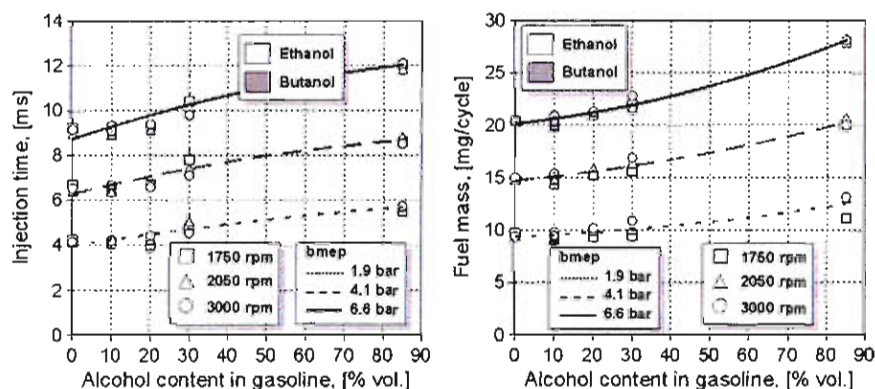
Fig. 2. Injection time and fuel mass injected per cycle bmep trend lines as a function of alcohol content.

of stoichiometric mixture ($H_{st.mix}$) is quite similar and therefore engine power is not affected by fuel composition. Some benefit could derive from mixture cooling effect due to the higher ethanol heat of vaporization (H_v). As a consequence some positive effect on volumetric efficiency is expected at ethanol percentage increasing. Moreover grams of CO_2 per MJ produced are not influenced by oxygenated compounds at the same engine efficiency. Due to molecule type very similar to gasoline composition, n-butanol has better fuel properties than ethanol [17]. It can be blended with gasoline at any percentage without modifying the engine. The energy content (H_i) is higher than ethanol and comparable to gasoline.

2.3. Emission sampling and characterization

For gaseous regulated emissions a hot ABB UV Limas 11 (ultra violet sensor) for nitrogen oxides (NOx), a cold ABB URAS 14 for

CO, CO_2 (infra-red sensor) and oxygen (electro-chemical cell), and a hot Beckman 404 FID analyzer (flame ionization detector) for THC were used.

Besides regulated emissions, also particles and some gaseous unregulated pollutants were investigated. All the unregulated pollutants were sampled downstream a double stage dilution device (Fine Particle Sampler – FPS by Dekati Ltd.) which diluted the engine-out raw gas almost 14 times with purified shop air at a temperature of almost 150 °C.

Particle number (PN) and size distribution were measured by an Electric Low Pressure Impactor (ELPI) by Dekati Ltd. It is able to count, in a continuous way, the number of particles with the aerodynamic diameter between 7 nm and 10 µm, collected on twelve dimensional stages. ELPI data were also used to estimate the particulate mass (PM). Considering the particles as spheres, the particle mass was evaluated assuming their density as 1 g/cm³. This
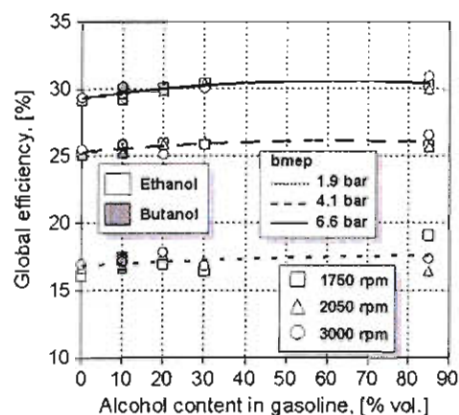
4

Fig. 3. Global efficiency bmep trend lines as a function of alcohol content.

statement represents a strong hypothesis on the density value which is a function of the particle diameter: higher the diameter, lower the density [18]. The mass calculation starting from the particle numbers could be affected by a great error, mostly for the larger particles that more account for the total volume and mass. In order to limit the inaccuracy, only mass of particles with the diameter lower than 1 µm (PM_1) was estimated.

Polycyclic Aromatic Hydrocarbons (PAHs) were collected by using the sorbent tubes XAD-2 by SKC, connected to a constant volume sampler Bravo H Plus by TCR Tecora (flow rate of almost

10 lpm). After sampling, the sorbent tubes were Soxhlet extracted with cyclohexane for at least 12 h with the addiction of the recovery standard mixture (Dr. Ehrenstorfer Mix 31), and then concentrated to 0.5 ml. PAHs analysis was realized with a gas chromatograph (HP 5890 Series II) coupled with a mass selective detector (HP 5971A) [19]. The chromatographic operative conditions and the internal standard analysis to quantify PAHs from phenanthrene to dibenzo(a,l)pyrene were reported in [20]. Table 2 lists all gaseous unregulated pollutants which were determined. The table indicates the pollutant group (PAHs, carbonylics and VOC) and the IARC (International Agency for Research on Cancer) classification for carcinogenicity [21].

Carbonylic compounds were collected by using the DNPH-cartridges by Waters connected to a sampling pump (flow rate of almost 4 lpm) and a volumetric counter. After sampling, the cartridges were chemically extracted with 3 ml of acetonitrile. Chemical analysis was realized with a HPLC (HP 1050) coupled with an ultraviolet detector [22]. The operative condition are: Supelco column LC-18 (25 cm × 4.6 mm × 5 µm); two mobile phases: A water/acetonitrile/tetrahydrofuran 60/30/10 v/v and B water/acetonitrile 40/60 v/v; constant flow rate of 1.5 ml/min; gradient conditions: 100% A for 1 min and then a linear gradient from 100% A to 100% B in 10 min. Five dilutions of the standard mixture TO11/IP-6A by Supelco were used for the quantitative analysis. Formaldehyde and acetaldehyde are classified by IARC as carcinogenic and probably carcinogenic to humans, respectively.

A chromatographic analysis was carried out directly on the gaseous sample for evaluating the volumetric concentration of some
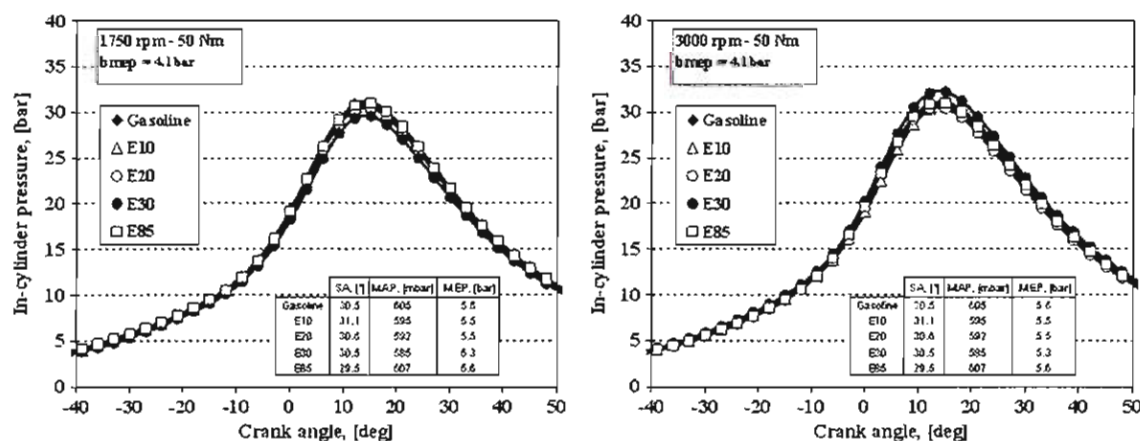
Fig. 4. In-cylinder pressure at 4.1 bmep load at 3000 and 1750 rpm for gasoline and all the tested oxygenated blends.
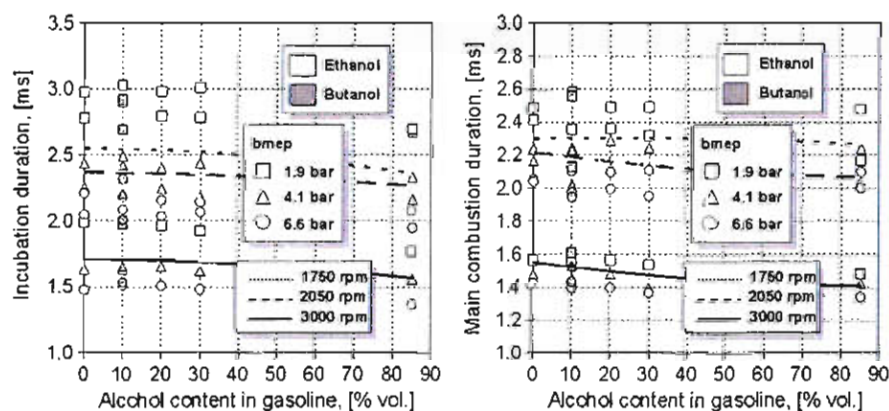
Fig. 5. Incubation and main combustion duration bmep trend lines as a function of alcohol content.
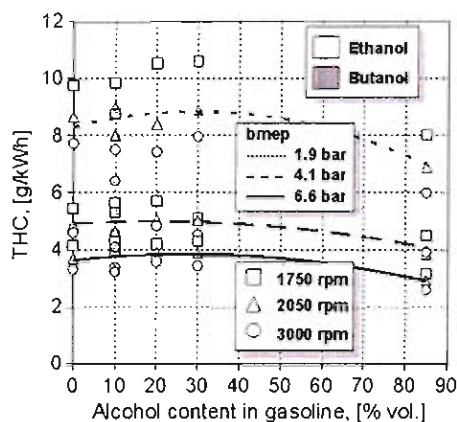
5

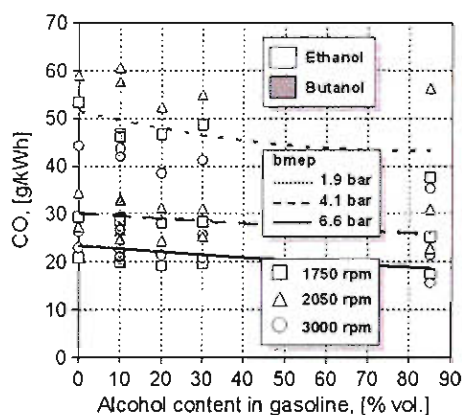**Fig. 6.** THC emissions upstream of the catalyst.

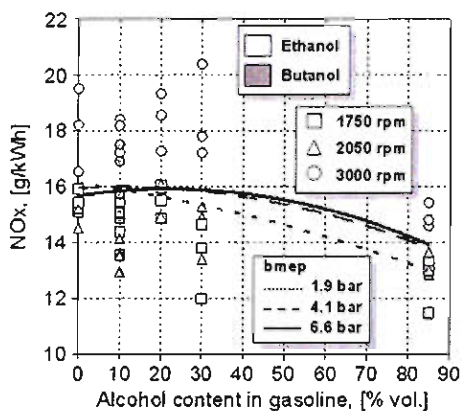**Fig. 7.** CO emissions upstream of the catalyst.

Fig. 8. NOx emissions upstream of the catalyst.

Volatile Organic Compounds (VOCs) with a carbon atoms number between C_1 and C_7. Among these, 1,3-butadiene and benzene cover a relevant role because of their carcinogenic potential (see Table 2). The gaseous sample was injected in the GC with flame ionization detector (FID) through a sample loop of 0.5 ml. The operative conditions are: carrier gas: helium; capillary column: Agilent HP-Al/ KCl 50 m × 0.55 mm × 15 µm; Initial head column pressure: 50 kPa; Injector temperature: 250 °C; Initial oven temperature: 80 °C; program of temperature: isothermal for 16 min, 10 °C/min up to 160 °C; 5 °C/min up to 180 °C; 2 °C/min up to 200 °C– 50 min at 200 °C. The calibration curves for quantitative analysis

were made with five dilutions of a certified gaseous mixture standard.

3. Results and discussion

3.1. Combustion analysis

A stoichiometric operation closed loop was assured by the Electronic Control Unit (ECU) in all tested steady states. Spark advance (SA) has been optimized to have the peak pressure at the same angle position (13–16° ATDC) for the different fuels, while the standard ECU showed a trend to reduce SA increasing the ethanol content. Anyway the spark advance optimization was very small (not higher than 3%). In these optimized conditions, any influence of ethanol content was observed on the manifold absolute pressure and exhaust temperature. Not great variations of the injection time and the fuel mass injected per cycle were noted up to E20, whereas with E30 and E85 a longer injection time was expected due to a lower energy content for mass unit and a relative quite constant density of high content ethanol blends. Fig. 2 reports three constant bmep (Brake Mean Effective Pressure) trend lines of injection time and fuel mass injected per cycle for all the engine speed and alcohol blends. In all the graphs of this paper, n-butanol data are distinguished by ethanol ones by using grey-filled indicators. At each bmep the increase is not depending by speed and it is more evident for E30 and E85.

The observed fuel mass increasing is appreciably lower than predictable one estimated from fuel properties. Experimental data were confirmed by using two different measuring devices (a Coriolis mass flow meter and a precision electronic balance), which gave the same results. The slightly better efficiency with E85 was also confirmed by a mean CO_2 improvement of 7% for E85 vs gasoline.

The global efficiency of E85 estimated from the lower heating values of Table 1 was 4% higher than that of gasoline (Fig. 3) even though the combustion efficiency did not change with the fuel. Therefore the efficiency improvement could be related to other parameters, such as a lower compression work (for lower intake temperatures) and lower thermal losses (for lower maximum in-cylinder temperatures). From these results a "tank to wheel" analysis should give a small CO_2 and consumption reductions in a conventional port injection spark ignition engine. Some effective benefits could derive if a positive global carbon balance from well to tank is achieved.

Combustion analysis carried out by measuring in cylinder pressure confirm that fuel does not influence combustion quality, not giving a reason to justify the engine efficiency improvement shown in Fig. 3. Combustion development was deeply analyzed at 50 Nm (bmep 4.1 bar) at 1750 rpm and 3000 rpm. In Fig. 4 in-cylinder pressure is represented in the "late/compression – combustion – early expansion" crank angle area for the five tested fuels at 4.1 bmep load at 3000 and 1750 rpm. With spark advance optimization in each operative conditions, no great differences among the pressure cycles of the five fuels can be observed.

Intake and exhaust pressure curves did not differ for the five tested fuels since also throttle angle is almost similar. Same behavior was observed for the burned mass fraction, being both incubation time of combustion and main duration combustion substantially the same for all the tested fuels, with the exception of E85 blend. Fig. 5 shows lower incubation and main combustion duration for E85, stating a slightly faster combustion with this blend. Also engine head thermal load does not significantly changes with oxygenated blends, in fact temperature measured in the area between inlet and exhaust valves is almost similar in each operating condition for all the tested fuels. Temperature vari-
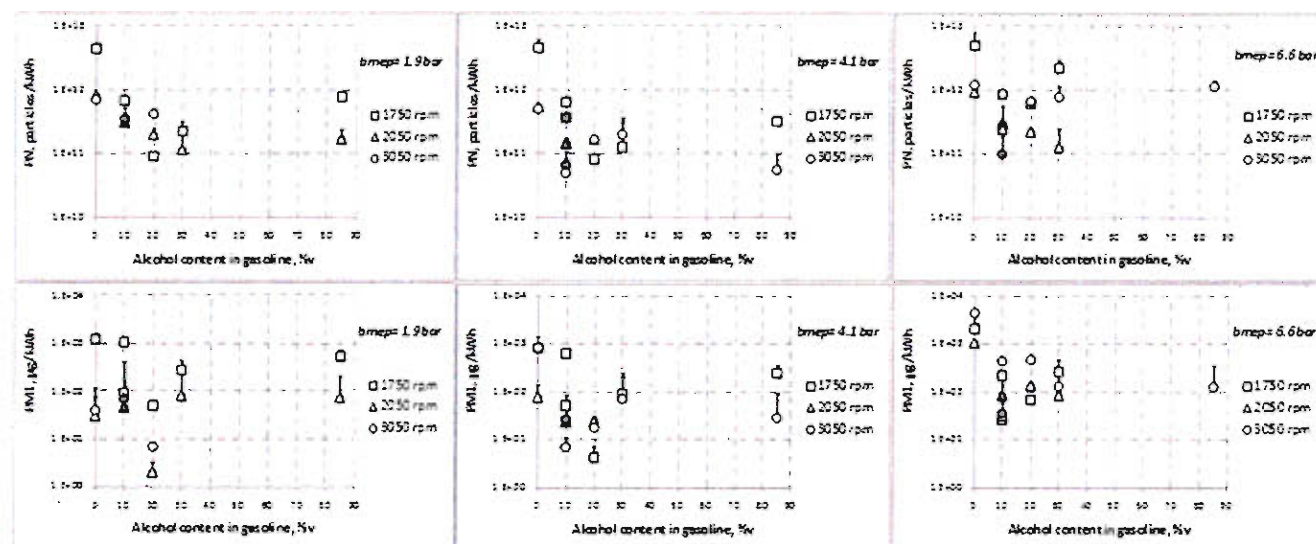
6

Fig. 9. PN and PM$_1$ emissions as a function of alcohol content.

ations are only related to the different speed/load operative conditions, but not to the fuel composition. These data are in accordance with pressure cycle development observed for the different fuels.

3.2. Emissions analysis at engine-out

3.2.1. Regulated emissions

In Figs. 6–8 regulated emission results (THC, CO and NOx) upstream the catalyst are shown in each experimental point as load trend line at the three tested speed.

Since FID sensibility towards HC coming from pure ethanol is reduced at 46% [23], measured THC concentration were increased proportionally to the ethanol and butanol fraction in blend (ranging from 10% to 85%) in each point of the experimental grid. For highest alcohol content, a small decreasing of THC was observed (Fig. 6). CO emissions follow alcohol content in the blends. This behavior can be justified by oxygen presence in the molecule, that should improve combustion quality and therefore give a reduction of CO at the exhaust (Fig. 7).

NOx behavior is quite similar to THC. The lower percentage measured (Fig. 8) at ethanol increasing levels is in accordance with higher vaporization heat, typical of oxygenated compounds, giving lower air/fuel mixture temperature at intake and, as a consequence, also lower peak temperatures in combustion chamber. The mixture temperature at intake valve, measured during experiments, is progressively lower with alcohol increasing in blends. The difference is quite small between several fuels, reaching the maximum value between gasoline and E85 (almost 4%); it could be due to the fact that only a small amount of fuel has vaporized into intake manifold, since a larger quantity should vaporize into the cylinder during intake and compression stroke.

3.2.2. Particulate matter characterization

PN and PM$_1$ emissions were measured at the engine exhaust with gasoline, n-B10 E10, E20 and E85. For each fuel type, an experimental test composed by all the engine experimental points was carried out. Fig. 9 shows PN and PM$_1$ mean values (expressed as particles/kW h and μg/kW h, respectively) in a semi-log graph as a function of the alcohol content in gasoline for the three tested engine loads (1.9, 4.1 and 6.6 bar as bmep). At the same engine load, PN emissions clearly decrease of almost one order of magnitude when moving from gasoline to E85. The PN reduction percentage of alcohol blends respect on gasoline ranges between 30% and

95% whereas the PM$_1$ one between 10% and 98%. The influence of engine speed is, instead, not so clear. It has to be noted that, for some fuel formulations and in correspondence of low load experimental points, PN become not measurable (i.e. lower than the ELPI Limit of Detection – LOD).

Fig. 10 represents the particle size distribution for the five fuel formulations over the several engine loads (1.9, 4.1 and 6.6 bar as bmep). For low and medium engine load, gasoline distribution is referred to secondary y axis, due to different values to be plotted.

99% of particle number distribution is included in PM$_1$ zone (particle diameter lower than 1 μm). The size distributions relative to gasoline are bimodal in almost all conditions; they, in fact, present a first peak in the ultra-fine dimensional zone (less than 20 nm) corresponding to the first ELPI collecting stage, and a second peak around 70 nm (3rd ELPI dimensional stage). The particle size distribution of alcohol blends are, instead, in most cases totally decreasing [24]. In other words, the main difference between gasoline and alcohol blends particle size distribution lies in the number of particles with the smallest diameter belonging to the nucleation mode; for gasoline, the contribution of these particles is stronger than for the tested oxygenated fuels. This observation agrees with the highest HC emissions related to gasoline fuel, which mainly constitutes the volatile particulate fraction included in the nucleation mode.

The different size distribution measured with pure gasoline and gasoline blends also justifies the different estimated reduction in PN and PM$_1$. These differences are explained by the major contribution of larger particles in particulate mass evaluation respect to the smaller ones.

3.2.3. Unregulated organic emissions

Emissions of carbonylic compounds, VOC and PAHs were measured with gasoline, n-B10, E10, E20, E30 and E85 over the high load engine experiments.

In Fig. 11 the emissions of carbonylic sum (expressed as mg/kW h) are reported as a function of alcohol content in gasoline for all experimental conditions. It is evident an increasing of carbonylics when alcohol percentage in gasoline increases. The carbonylic increment is not dependent by engine speed conditions and it is stronger for E85 blend. For n-B10, E10, E20 and E30, the carbonylic sum is, in fact, almost twice that of gasoline; for E85 this ratio becomes almost 3.5. The aldehydes increasing was already observed by [25].
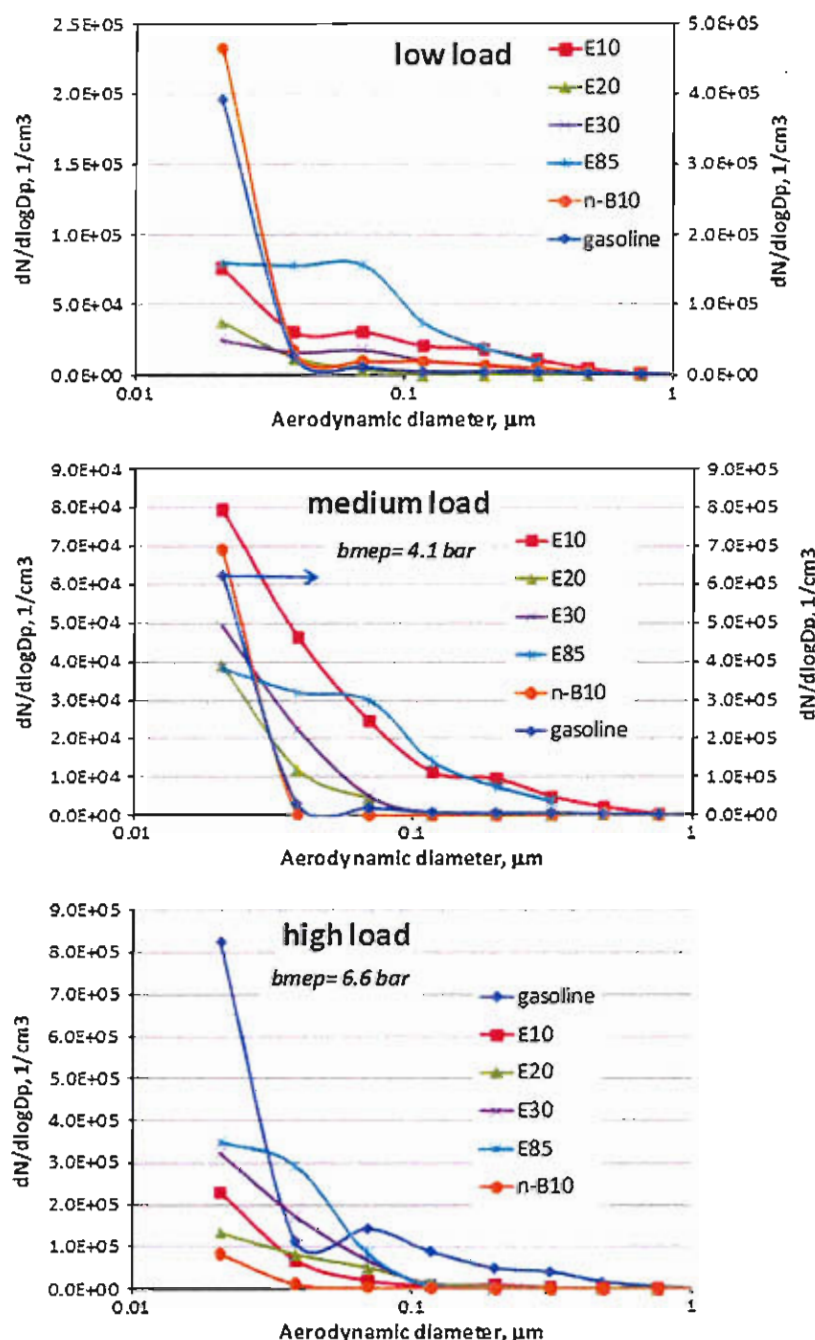
7

Fig. 10. Particle size distribution.

Fig. 12 reports the speciation of carbonylic compounds. These data are obtained by averaging the emissions measured over 1750–2050–3000 rpm/80 Nm with the same fuel. In all the conditions, the measurable compounds range from formaldehyde to benzaldehyde, in agreement with [26]. The most abundant compounds are formaldehyde and acetaldehyde whose sum covers almost 85% of total. They are followed, as abundance, by benzaldehyde and acetone. The strong increment of carbonylic sum observed for E85 blend is due to acetaldehyde whose emissions become much higher than those relative to the other fuels [27].

The mass percentage of total carbonylics in THC measured by FID analyzer is almost 3% for gasoline fuel, almost 8% n-B10, E10, E20 and E30 fuels and reaches almost 14% for E85.

Sum of VOCs is plotted as a function of the alcohol content in Fig. 13. Data are grouped for the several engine speeds. It is evident

a marked reduction for E85 blend (between 50% and 70% compared with gasoline). Two ranges of values are in fact evident: the first between 1500 and 2000 mg/kW h which includes gasoline, n-B10, E10, E20 and E30, and the second between 700 and 1000 mg/kW h referred to E85. The decreasing trend is already visible for E30, even though the reduction percentage is almost 5–10% compared with gasoline emissions.

According to the average VOC speciation (Fig. 14), the most abundant compounds are ethylene and acetylene, followed by methane and propylene. Total quantified VOCs constitute almost 50% of THC measured with FID for gasoline, n-B10, E10 and E20. This percentage decreases to almost 40% for E30 and almost 30% for E85. These percentages are different probably due to increasing carbonylic contribution with increasing alcohol content, taken into account for THC evaluation and obviously not considered in VOC sum. The carcinogenic compounds belonging to VOC list are

8
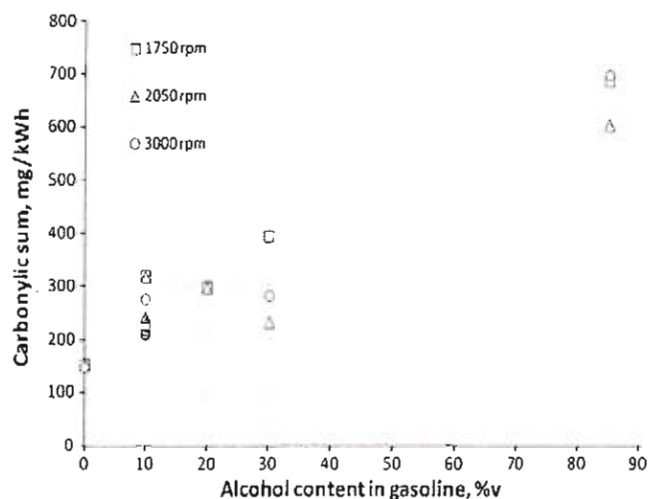
Fig. 11. Carbonylic compounds emissions as a function of alcohol blends.
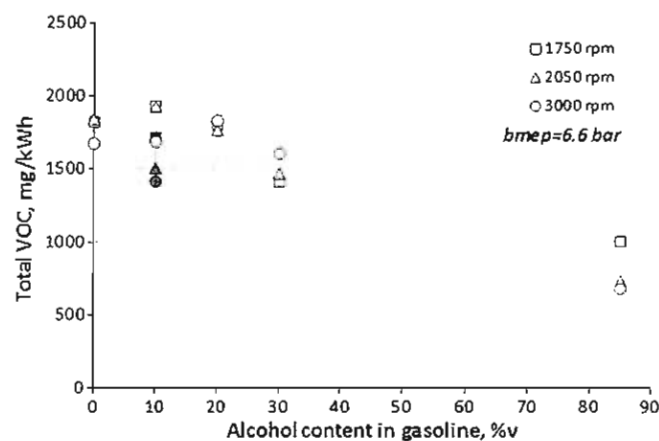
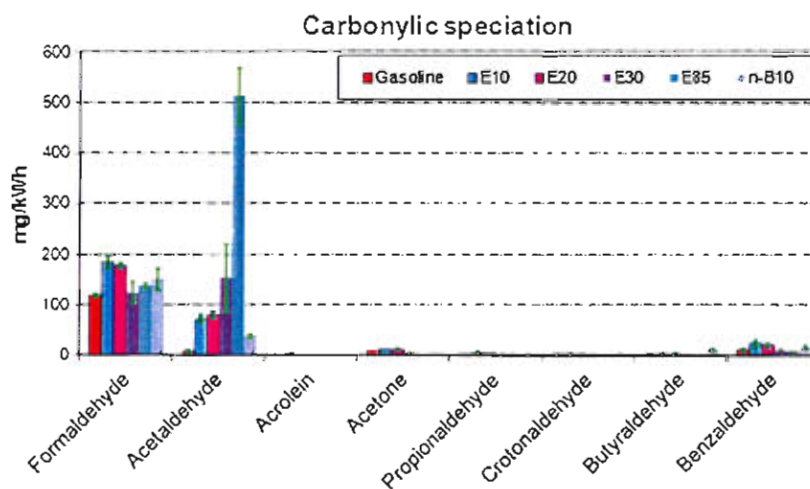**Fig. 13.** VOC emissions as a function of alcohol blends.

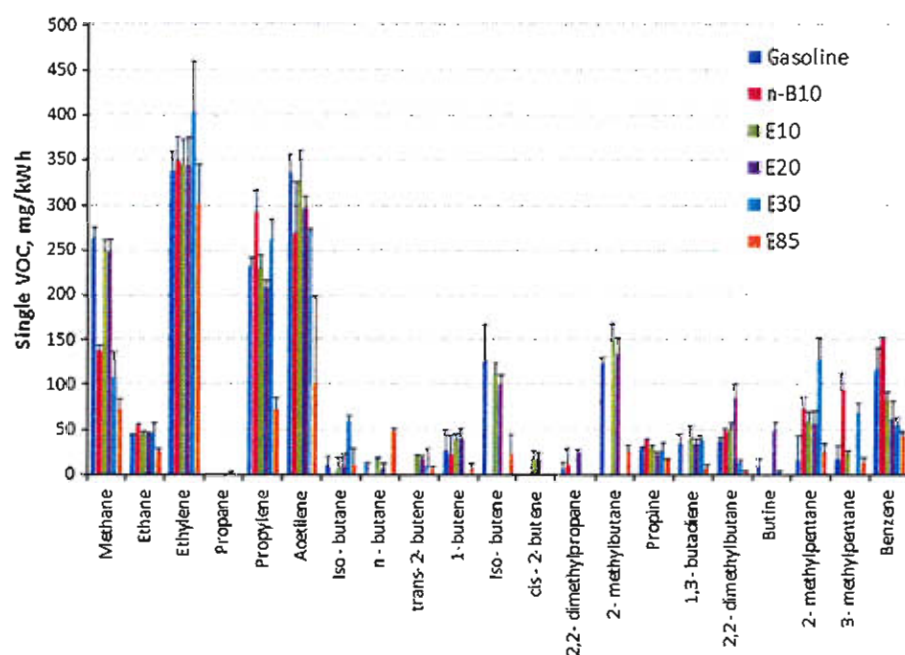**Fig. 12.** Carbonylic compounds speciation.
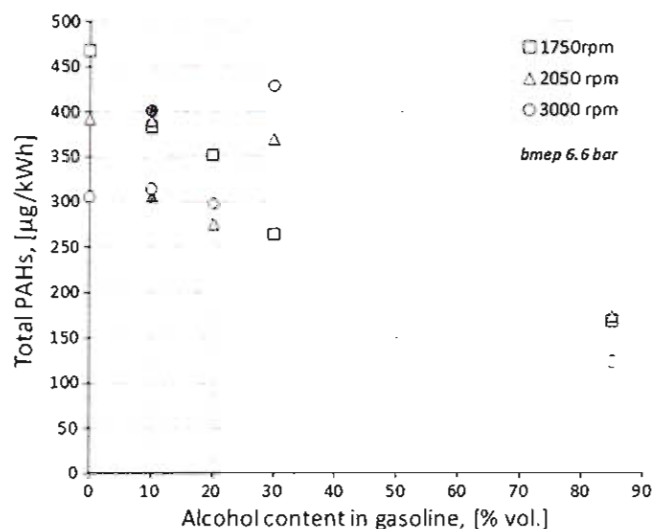

Fig. 14. VOC speciation.

9

Fig. 15. PAHs emissions vs alcohol content in gasoline.

1,3-butadiene and benzene. The emissions of 1,3-butadiene are lower than those of benzene, and also for these single compounds the reduction is clear for E85 blend.

The sum of PAH expressed as μg/kW h and measured over all experimental points, is summarized in Fig. 15 as a function of alcohol content in gasoline. The PAHs trend showed in this figure is very similar to THC ones (see Fig. 6); for an alcohol content between 0 and 30 vol%, PAHs, in fact, range between 250 and 450 μg/kW h, not showing a clear influence by alcohol content. When looking at emissions referred to same fuel, in fact, the variability associated to the average value does not allow to point out any significant difference. Emissions referred to E85, instead, are almost 150 μg/kW h, stating a marked reduction (from 40% to 70%) respect on the results obtained with the other alcohol/gasoline blends.

Fig. 16 specifies the composition of the PAHs sum, above discussed. It appears that no differences due to fuel type can be highlighted. Major constituent are the lightest compounds (from phenanthrene to pyrene). This is explained by the sampling procedure used during this experimental program. PAHs in fact were collected in the exhaust gas phase, mainly containing the light fraction (from 2 to 4 aromatic rings) of PAHs. The heavier fraction
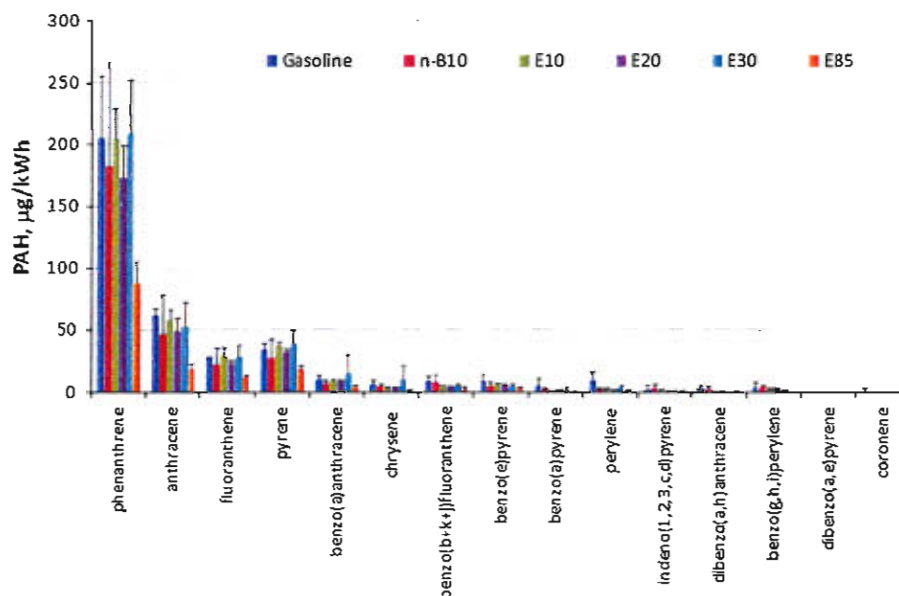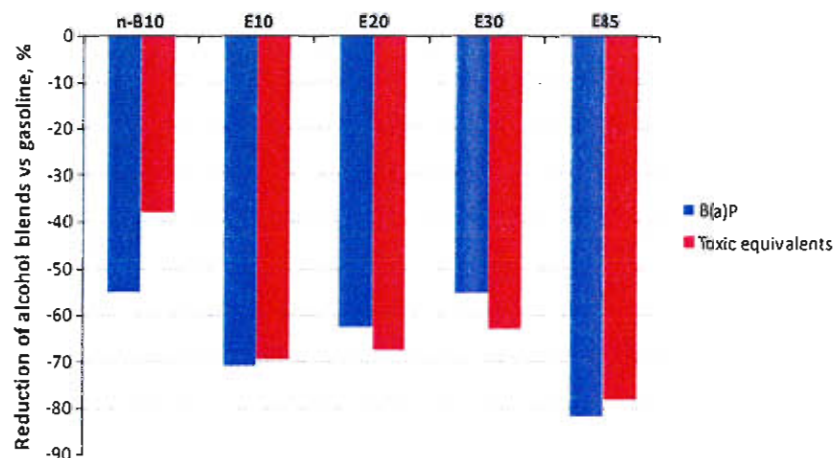

Fig. 16. PAHs speciation.

Fig. 17. B(a)P and toxic equivalents percentage reduction of alcohol blends compared to gasoline.

10

is typically associated to the particulate phase. The sum of carcinogenic PAHs (i.e. PAHs classified as belonging to IARC group 1, 2A and 2B) covers between 5% and 12% of total PAHs.

Benzo(a)pyrene (B(a)p), classified as carcinogenic to humans by IARC, is used as a marker for the carcinogenic risk of PAHs. The Individual PAH method (IPM) estimates a toxic equivalent (TEQ) by summing the emission levels of each aromatic expressed as "B(a)P equivalents". These last quantities are calculated by multiplying the concentration of single PAH for the carcinogenic potency relative to benzo(a)pyrene [28], the so called toxic equivalency factor – TEF. This method applied to PAHs experimental results provides a sensible reduction of toxic equivalents when moving from gasoline to alcohol blends. Fig. 17 reports the reduction percentage of toxic equivalents and benzo(a)pyrene (B(a)P) of alcohol blends compared to gasoline. Both reductions are strong (between 40% and 80%) with E85 showing the greatest percentage.

4. Conclusions

A deep experimental campaign was carried out to study the effect of gasoline/alcohol blends on performance and emissions of a 1.6 port injection spark ignition engine. Comparison between five fuel formulations was realized by modifying the spark advance in order to have an unchanged pressure peak position. In these operative conditions, the standard ECU was able to control air/fuel composition retaining the target stoichiometric value; therefore the engine was run in closed loop condition for all the tested fuels. No appreciable differences in combustion development were found, while a slightly better global efficiency (about +5% as mean values) was achieved with E85. As regard regulated emissions, the alcohol blends generally provide emission reduction respect on gasoline. The strongest reduction is associated to E85 (-20% for THC and about -15% for CO and NOx).

A significant reduction of PN and PM_1 (almost 90%) was achieved with alcohol blends compared to gasoline. Besides particle size distribution is always included in PM_1 dimensional range, distribution referred to oxygenated blends highlights a lower contribution of ultra-fine particles (aerodynamic diameter lower than 20 nm) in agreement with a lower volatile fraction.

The use of oxygenated fuels provides high carbonylic compound emissions; the strong increment compared to gasoline (almost 3.5 times higher) was measured for E85 blend and is mainly due to acetaldehyde. For alcohol content ranging between 10 and 30 vol%, the carbonylic sum becomes almost twice that of gasoline.

A 50% reduction of benzene and 1,3-butadiene emissions, classified as carcinogenic to humans was achieved with E85 blend.

Concerning PAHs, B(a)P and toxic equivalent evaluated for alcohol/gasoline blends reduce between 30% and 70% compared to gasoline. Also for this class of compounds, the best result in terms of PAHs emission reduction is obtained with E85 blend.

Acknowledgements

References

[1] He BQ, Hao JM, Yan XG, Xiao JH. A study on emission characteristics of an EFI engine with ethanol blended gasoline fuels. Atmos Environ 2003;37:949–57.

[2] Al-Hasan M. Effect of ethanol-unleaded gasoline blends on engine performance and exhaust emission. Energy Convers Manage 2003;44:1547–61.

[3] Schifter I, Diaz L, Rodriguez R, Gómez JP, Gonzalez U. Combustion and emissions behavior for ethanol–gasoline blends in a single cylinder engine. Fuel 2011;90:3586–92.

[4] Eyidogan M, Ozsezen AN, Canakci M, Turkcan A. Impact of alcohol–gasoline fuel blends on the performance and combustion characteristics of an SI engine. Fuel 2010;89:2713–20.

[5] Irimescu A. Performance and fuel conversion efficiency of a spark ignition engine fueled with iso-butanol. Appl Energy 2012;96:477–83.

[6] L-bin Wen, Xin C-Y, Yang S-C. The effect of adding dimethyl carbonate (DMC) and ethanol to unleaded gasoline on exhaust emission. Appl Energy 2010;87(1):115–21.

[7] Topgul T, Yucesu H, Cinar C, Koca A. The effects of ethanol–unleaded gasoline blends and ignition timing on engine performance and exhaust emissions. Renewable Energy 2006;31:2534–42.

[8] Visakhamoorthy S, Wen JZ, Sivoththaman S, Koch CR. Numerical study of a butanol/heptane fuelled homogeneous charge compression ignition (HCCI) engine utilizing negative valve overlap. Appl Energy 2012;94:166–73.

[9] Maurya RK, Agarwal AK. Experimental study of combustion and emission characteristics of ethanol fuelled port injected homogeneous charge compression ignition (HCCI) combustion engine. Appl Energy 2011;88(4):1169–80.

[10] Wu X, Daniel R, Tian G, et al. Dual-injection: the flexible, bi-fuel concept for spark-ignition engines fuelled with various gasoline and biofuel blends. Appl Energy 2011;88(7):2305–14.

[11] Daniel R, Xu H, Wang C, Richardson D, Shuai S. Combustion performance of 2,5-dimethylfuran blends using dual-injection compared to direct-injection in a SI engine. Appl Energy 2012;98:59–68.

[12] Niven RK. Ethanol in gasoline: environmental impacts and sustainability review article. Renew Sustain Energy Rev 2005;9:535–55.

[13] Liu FJ, Liu P, Zhu Z, Wei YJ, Liu SH. Regulated and unregulated emissions from a spark-ignition engine fuelled with low-blend ethanol–gasoline mixtures. Proc Inst Mech Eng D – J Automob Eng 2012;226(4):517–28.

[14] Yang HH, Liu TC, Chang CF, Lee E. Effects of ethanol-blended gasoline on emissions of regulated air pollutants and carbonyls from motorcycles. Appl Energy 2012;89:281–6.

[15] Chen L, Stone R, Richardson D. A study of mixture preparation and PM emissions using a direct injection engine fuelled with stoichiometric gasoline/ethanol blends. Fuel 2012;96:120–30.

[16] Gu X, Huang Z, Cai J, Gong J, Wu X, Lee C. Emission characteristics of a spark-ignition engine fuelled with gasoline-n-butanol blends in combination with EGR. Fuel 2012;93:611–7.

[17] Szulczyk KR. Which is a better transportation fuel – butanol or ethanol? Int J Energy Environ 2010;1(3):501–12.

[18] Schmi O, Karg E, Hagen DE, Whitefield PD, Ferron GA. On the effective density of non-spherical particles as derived from combined measurements of aerodynamic and mobility equivalent size. J Aerosol Sci 2007;38(4):431–43.

[19] US-EPA-US. Environmental protection agency. Compendium Method TO-13A-Determination of Polycyclic Aromatic Hydrocarbons (PAHs) in Ambient Air Using Gas Chromatography/Mass Spectrometry (GC/MS); 1999 [EPA/625/R-96/010b].

[20] Seggiani M, Prati MV, Costagliola MA, Puccini M, Vitolo S. Bioethanol – gasoline fuel blends: exhaust emissions and morphological characterization of particulate from a moped engine. J Air Waste Manag Assoc 2012;62(8):888–97.

[21] IARC (International Agency for Research on Cancer). IARC monographs on evaluation of carcinogenic risks to humans, overall evaluation of carcinogenicity: an updating of monographs. IARC Monogr. Eval. Carcinog. Risk Chem Hum. Lyon, France; 1987.

[22] US-EPA-US. Environmental protection agency. Compendium Method TO-11 – Determination of Formaldehyde in Ambient Air Using Adsorbent Cartridge Followed by High Performance Liquid Chromatography (HPLC); 1999.

[23] Sandstroem-Dahl C, Erlandsson L, Gasste J. METEV, Measurement Technology for Emissions from Ethanol Fuelled Vehicles AVL MTC 9711, AVL MTC AB 2009/11; 2009.

[24] Lee H, Myung CL, Park S. Time-resolved particle emission and size distribution characteristics during dynamic engine operation conditions with ethanol-blended fuels. Fuel 2009;88:1680–6.

[25] Poulopoulos SG, Samaras DP, Philippopoulos CJ. Regulated and unregulated emissions from an internal combustion engine operating on ethanol-containing fuels. Atmos Environ 2001;35:4399–406.

[26] Pang X, Mu Y, Yuan J, Hea H. Carbonyls emission from ethanol-blended gasoline and biodiesel-ethanol-diesel used in engines. Atmos Environ 2008;42:1349–58.

[27] Graham LA, Belisle SL, Baas C. Emissions from light duty gasoline vehicles operating on low blend ethanol gasoline and E85. Atmos Environ 2008;42:4498–516.

[28] MOE (Ministry of the Environment). Scientific criteria document for multimedia standards development. Polycyclic Aromatic Hydrocarbons (PAH). Part1: Hazard Identification and Dose-Response Assessment. Ministry of the Environment. Toronto (Ontario); 1997.
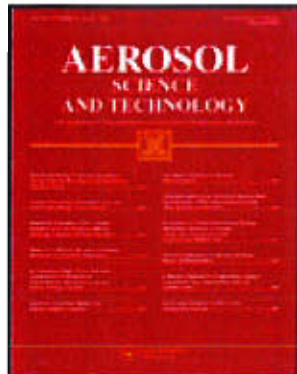
The Impact of Ethanol Fuel Blends on PM Emissions from a Light-Duty GDI Vehicle

M. Matti Maricq [a], Joseph J. Szente [a] & Ken Jahr [a]

[a] Research & Advanced Engineering, Ford Motor Company, Dearborn, Michigan, USA

PLEASE SCROLL DOWN FOR ARTICLE

The Impact of Ethanol Fuel Blends on PM Emissions from a Light-Duty GDI Vehicle

M. Matti Maricq, Joseph J. Szente, and Ken Jahr
Research & Advanced Engineering, Ford Motor Company, Dearborn, Michigan, USA

This study explores the influence of ethanol on particulate matter (PM) emissions from gasoline direct injection (GDI) vehicles, a technology introduced to improve fuel economy and lower CO_2 emissions, but facing challenges to meet next-generation emissions standards. Because PM formation in GDI engines is sensitive to a number of operating parameters, two engine calibrations are examined to gauge the robustness of the results. As the ethanol level in gasoline increases from 0% to 20%, there is possibly a small (<20%) benefit in PM mass and particle number emissions, but this is within test variability. When the ethanol content increases to >30%, there is a statistically significant 30%–45% reduction in PM mass and number emissions observed for both engine calibrations. Particle size is unaffected by ethanol level. PM composition is primarily elemental carbon; the organic fraction increases from ~5% for E0 to 15% for E45 fuel. Engine-out hydrocarbon and NO_x emissions exhibit 10–20% decreases, consistent with oxygenated fuel additives. These results are discussed in the context of the changing commercial fuel and engine technology landscapes.

[Supplementary materials are available for this article. Go to the publisher's online edition of *Aerosol Science and Technology* to view the free supplementary files.]

INTRODUCTION

Three areas related to motor vehicles and air quality are experiencing major changes. The first is fuel composition. Recent energy policy decisions, such as the 2007 Energy Independence and Security Act, mandate increased reliance on renewable fuels, directives to enhance national security and ameliorate climate change impacts (U.S. Environmental Protection Agency 2007). This implies increased blending of ethanol into conventional gasoline fuel. Roughly 90% of gasoline sold in the

United States currently contains nearly 10% ethanol (E10) (U. S. Energy Information Administration 2011). This will increase following the United States Environmental Protection Agency (EPA) partial waiver to allow E15 fuel use in 2007+ model year vehicles (U. S. Environmental Protection Agency 2010).

The second is the growth of gasoline direct injection (GDI) engine technology, aimed to offer fuel economy and CO_2 emissions benefits (Fraser et al. 2009; Yi et al. 2009). Direct injection of gasoline into the cylinder allows better combustion control, for example, multiple fuel injections and charge-air cooling. But it risks incomplete fuel volatilization and impingement onto piston and cylinder surfaces, exacerbating particulate matter (PM) emissions. The third is regulatory; California Air Resources Board (ARB) and EPA are both contemplating next-generation emissions standards which would lower tailpipe PM emissions from 10 mg/mi to 6 mg/mi, and then 3 mg/mi, over the next decade (California Air Resources Board 2010).

Consequently, it is important to examine the interplay and potential synergies between fuel composition and engine technology in efforts to reduce emissions. There are ongoing investigations of ethanol's effects on fuel systems, evaporative emissions, and gaseous emissions (Durbin et al. 2007; Kar and Cheng 2009; Knoll et al. 2009; Coordinating Research Council 2011), but few gasoline engine studies have examined its impact on PM emissions. The paucity of data is presumably because stoichiometric combustion in spark ignition engines naturally produces very low PM emissions, a few milligrams per mile (Maricq et al. 1999), and because GDI is a new technology. One exception is the effort by Aikawa et al. (2010) to create a PM index based on fuel properties, which is of interest for GDI because of the potential to help model air fuel mixing and sooting propensity.

Ethanol effects on GDI particulate emissions have been reported by Storey et al. (2010) and He et al. (2010), who observed reductions of about 30% for E20 fuel over the Federal Test Procedure (FTP) drive cycle. However, the detailed characterizations, such as particle number, size, and composition, were undertaken at steady-state engine operation, whereas cold and hot starts and transients are typically of more interest for gasoline engines. Work by Chen et al. (2010) showed that PM

emissions can either increase or decrease with ethanol content depending on fuel injection timing. Such results point out a difficulty in investigating potential fuel benefits, namely that these might be masked by adjustments in engine calibration when the fuel is changed. Other properties of fuel besides ethanol content can also impact PM emissions; thus, Khalek et al. (2010) noted higher PM levels from a GDI vehicle operated on a commercial E10 fuel relative to two E0 fuels, but attributed this to a higher volatility in the base gasoline.

The goal of this paper is to examine how ethanol–gasoline blends impact PM emissions from GDI vehicles. Six fuels are examined, ranging from E0 (base gasoline) to E45 (45% ethanol). The study utilizes the FTP drive cycle to include the important effects of cold start and transient operation. It addresses measurement variability both by repeat tests and the use of three metrics of PM emissions: mass, number, and elemental/organic carbon composition. The issue of sensitivity to engine parameters is handled in two ways: First, we conduct testing at two different engine calibrations to assess the consistency of ethanol's impact on emissions. Second, we compare the vehicle exhaust results to observations from a study of ethanol–gasoline blend diffusion flames (Maricq 2011).

TABLE 1
Fuel properties

Characteristic	E0	E10 cert	E10 pump	E100
Ethanol (%vol)	0	10.1	9.0	97.3
10% recovery dist. T (°C)	56.7	54.8	48.5	
50% recovery dist. T (°C)	105.6	98.4	69.8	
90% recovery dist. T (°C)	155.8	158.8	165.5	
Density (g/mL)	0.744	0.754	0.734	0.795
Vapor pres. ASTM (kPa)	55.2	54.5	70.6	21.0
Net heating value (MJ/kg)	43.34	41.5		26.73
Research octane	97.3	94.4	91.8	
Carbon weight%	86.41	82.90		52.16
Hydrogen weight%	13.59	13.41		13.08
Oxygen weight%	<0.05	3.69		34.76
Sulfur (ppm)	19	5	58.8	3
Aromatics (%vol)	28.5	24.1	16.9	

EXPERIMENTAL METHODS

Test Vehicle and Fuels

The test vehicle is a light-duty truck equipped with a 3.5-L V6 gasoline turbocharged direct injection engine. It is representative of current GDI products, but contains prototype elements, such as the engine calibrations tested here. It has a compression ratio of 9.8:1 and independent variable cam timing. The fuel injectors are side-mounted and deliver single-fuel pulses, except for split injection (two pulses) during crank and early cold start operation. Exhaust aftertreatment consists of a three-way catalyst to control hydrocarbon (HC) and NO_x emissions.

The study uses four fuels: certification test gasoline (E0), a commercial E10 fuel similar to that expected for future certification, a commercial pump grade E10, and a commercial E100 fuel used for blending. Their properties are listed in Table 1. E100 and E0 were splash-blended to produce the E17, E32, and E45 fuels. All fuels were analyzed by gas chromatography to verify ethanol content. Fuel changes were done by draining the tank, filling with new fuel, and running the vehicle through the FTP drive cycle prior to testing. Emissions were measured over the FTP cycle, consisting of three phases: (1) cold start, (2) urban, and (3) hot start. E0 tests were conducted first and last to confirm that no changes in vehicle emissions performance occurred.

PM Sampling and Measurement

The vehicle was tested on a 48-inch single roll, AC electric, chassis dynamometer. The experimental setup is illustrated in Figure 1. Vehicle exhaust was sampled in two ways: (1) directly

from the tailpipe and (2) through a full-flow constant volume sampling (CVS) dilution tunnel, as per the regulatory method (except to substitute quartz filter EC/OC analysis for Teflo filter gravimetric PM mass). In our CVS system, exhaust is diluted with a "remote mix T" connected to the tailpipe via a short (~1 m) extension. The dilution air is filtered, temperature- and humidity-controlled (38°C and −9°C dew point), and actively regulated to maintain a constant total flow of exhaust plus dilution air. This was set to 9.34 m³/min for E0, E10, and E17 fuels, but raised to 19.8 m³/min for E32 and E45 because of increased exhaust humidity. The diluted exhaust travels via a ~7-m, 25.4-cm-diameter, conductive coated Teflon tube to a 30.4-cm-diameter stainless steel tunnel.

Direct tailpipe sampling employs a Dekati Fine Particle Sampler (FPS) originally developed to provide standardized dilution conditions for studying nucleation mode formation (Ntziachristos and Samaras 2010). It uses a coaxial perforated tube diluter that allows room temperature dilution, but avoids thermophoretic deposition of PM from hot exhaust. This approach contrasts with the European Union solid particle counting method, which is designed to remove nucleation mode particles by hot dilution and evaporation (Giechaskiel et al. 2008). Instead, the FPS samples both semivolatile and solid particles. It was used at a dilution factor of 25–30. A Dekati ejector pump provides 8.5 times secondary dilution for particle number counting. Room temperature nitrogen from liquid boil-off supplies the diluent for both the FPS and the ejector pumps.

Three PM emissions metrics are examined: (1) mass, (2) elemental/organic carbon (EC/OC), and (3) total particle
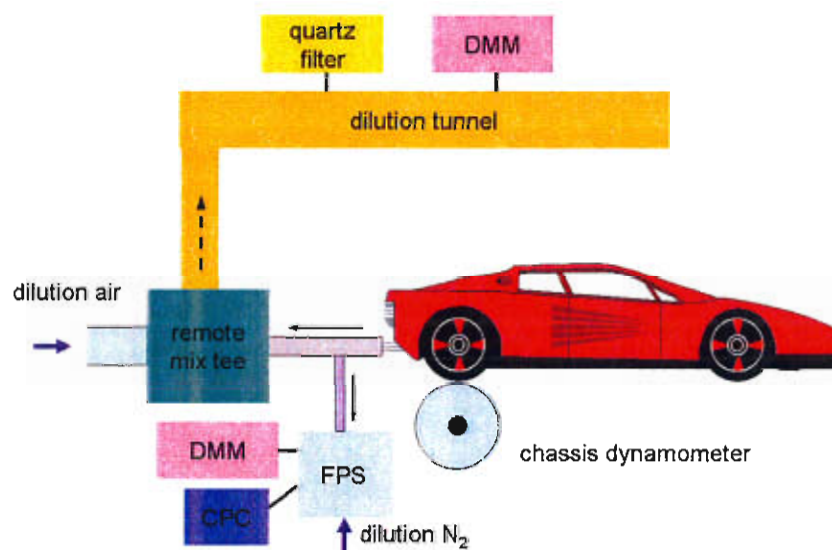
FIG. 1.   Schematic diagram of the experimental setup. Solid arrows show exhaust and diluent flows. Dashed arrow indicates diluted exhaust flow. (Color figure available online).

number. Engine-out HC and NO_x emissions are also reported. They are measured using Horiba analyzers based on flame ionization detection (FID) and chemiluminescence detection, respectively.

PM mass is determined by Dekati Mass Monitor (DMM) using a combination of electrical mobility and aerodynamic particle size measurements (Mamakos et al. 2006). Particles are charged in a corona discharge, segregated by mobility ($D_{50} = 50$ nm), and those penetrating the mobility classifier enter a cascade impactor. The resulting electrical currents and aerodynamic and mobility size information yield estimates for the quantity, volume, and effective density of particles, which are combined to calculate second-by-second PM mass concentration. Two DMMs were used, one at the tailpipe and the second at the CVS tunnel.

EC/OC particulate mass is determined by sampling diluted exhaust through prebaked 47-mm-diameter quartz filters, followed by thermal analysis with a Horiba MEXA 1370PM (Akard et al. 2004). The filters are heated to 980°C, first under nitrogen and then with oxygen present. CO_2 from the oxidation of material evolved under nitrogen is equated with organic carbon, whereas that produced with oxygen is attributed to elemental carbon. The OC mass includes a correction for hydrogen content assuming an H/C ratio of 1.85. A correction is also made for gas phase adsorption, which amounts to about 0.5 mg/mi (Maricq et al. 2011). Unlike the IMPROVE and NIOSH methods (Chow et al. 2001), there is no correction for pyrolysis, which impacts interpretation of EC/OC values. But the total PM mass compares well with gravimetric data (Akard et al. 2004).

Total particle number concentration is measured via TSI 3010 CPC (condensation particle counter). The lower size cutoff, 50% count efficiency, is 12 nm. This is nearly a factor of two smaller than the 23-nm cutpoint adopted by the EU for their solid particle method. The CPC counting efficiency at 70 and 100 nm was calibrated by electrometer to 100%.

Many of the E0 and E10 tests included tailpipe PM measurements by an electrical low-pressure impactor (ELPI) (Keskinen et al. 1992). This is a cascade impactor that measures second-by-second aerodynamic size distributions by first charging the particles in a corona discharge and then recording the electrical currents from the impactor stages. Previous work has shown that analysis of diesel particulate matter ELPI data using a fractal-like effective density results in PM mass and geometric mean mobility diameter estimates in good agreement with gravimetric and scanning mobility particle sizer data (Maricq et al. 2006).

RESULTS

Four engine calibrations (engine computer control of fuel pressure, fuel injection and spark timing, etc.) were initially examined with E0 fuel and found to have FTP cycle-weighted average PM emissions in the range of 3–7 mg/mi. Two of these near the proposed 3 mg/mi LEV III standard were selected for further study, labeled A and B. These differ in that calibration A produces lower cold start but higher urban and hot start PM relative to calibration B. Three to four repeat tests were performed with calibration A for each fuel; whereas, one to three were conducted with calibration B. The calibrations were not altered between fuels, except to adjust the amount of fuel needed to maintain a stoichiometric air/fuel ratio. The two calibrations show similar PM emissions trends with ethanol level; therefore, calibration A data are presented next, whereas those for calibration B are included in Supplementary Information.
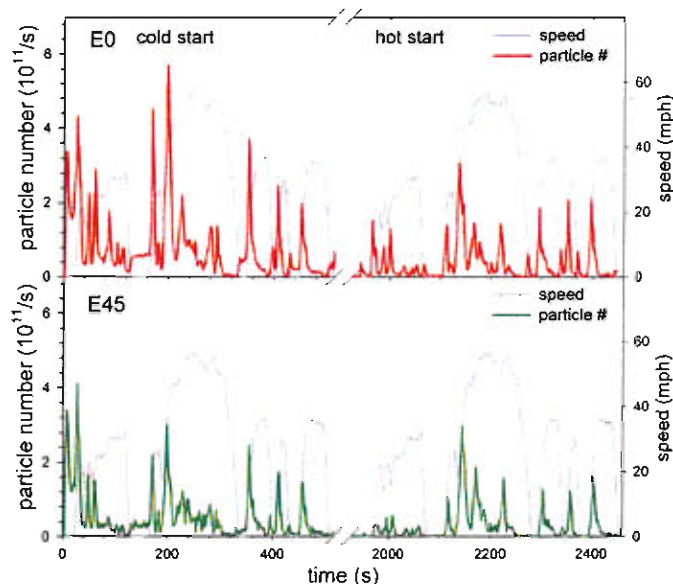
FIG. 2. Transient particle number emissions from the GDI test vehicle for the cold and hot start phases of the FTP drive cycle. Data are recorded by direct tailpipe sampling. Top panel: E0 fuel. Bottom panel: E45 fuel. (Color figure available online).

PM Mass and Number Emissions

Figure 2 illustrates tailpipe particle number emission rates over the cold and hot start FTP phases. Mass emissions (Figure S2 in Supplementary Information) exhibit a similar pattern.

When measured at the tailpipe, the particle concentrations recorded by DMM or CPC are multiplied by the time-aligned exhaust flow volume to derive emissions rates. Concentrations recorded via CVS sampling are simply scaled by the dilution tunnel flow. Not surprisingly, PM emissions correlate with vehicle acceleration owing to the increased fueling. But one also observes smaller emissions peaks during decelerations, likely a consequence of fuel shut-off. Emissions with E45 fuel are consistently below those for E0, but the decrease is not uniform, as seen from the accentuated reduction in particle emissions at the beginning of the hot start.

The effect of ethanol on PM emissions is summarized by Figures 3 and S3. These portray five parallel measurements: (1) mass from the tailpipe DMM, (2) mass from CVS tunnel DMM, (3) EC/OC mass from CVS, (4) particle count at tailpipe, and (5) ELPI PM mass for a subset of tests. The 1σ error bars represent test-to-test variability. Differences between the five methods reflect measurement uncertainty. This includes both systematic and random effects, but the data scatter points to random noise as the major contributor at these low emissions levels. The variability between the five PM methods is comparable to test-to-test variability in any given method. No statistically significant differences are observed between direct tailpipe and CVS sampling.
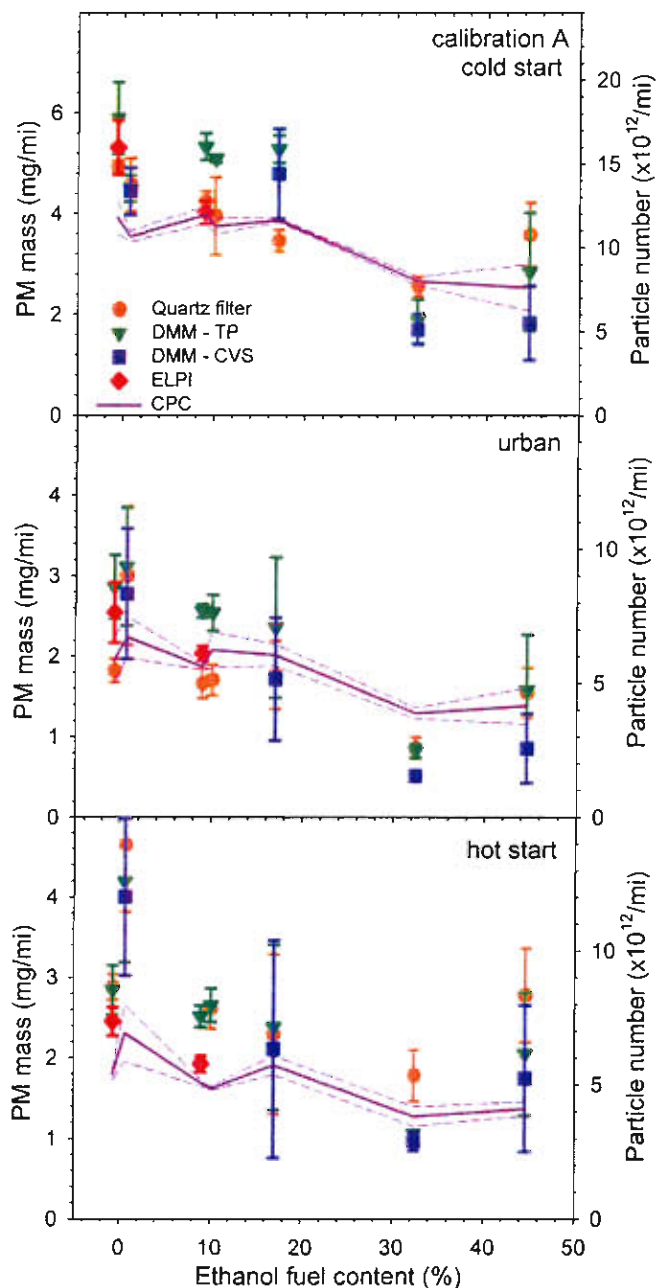

FIG. 3. GDI vehicle exhaust particle number and mass emissions versus ethanol content of fuel. Emissions are measured over the three-phase FTP drive cycle using calibration A. Symbols = mass. Lines = particle number. E0 data recorded at the beginning and end of the study are distinguished by plotting them slightly below and above 0% ethanol, respectively. Error bars are 1σ of the test repeatability. (Color figure available online).

All three metrics indicate a statistically significant reduction in particulate emissions with E32 and E45 fuels compared to base gasoline, relative to the average measurement uncertainty of approximately ±0.7 mg/mi. The decrease from E0 to these fuels is on average $\sim30\%$ by particle number and $\sim45\%$ by mass. This distinction is likely within the uncertainty, but could also

580   M.M. MARICQ ET AL.

originate from differences in nuclei mode particle emissions. Since E85 fuel further reduces PM (not part of this study), the small increase from E32 to E45 is likely from vehicle variability.

Figures 3 and S3 suggest a small (~20%) PM benefit for the lower ethanol blends relative to E0, but the data are mixed. Averaged over the parallel measurements, PM mass decreases 10–30% from E0 to E10 fuel using calibration A, but then remains constant from E10 to E17. For calibration B, there is a 10–20% PM increase from E0 to E10, but a ~10% decrease from E0 to E17 fuel. However, the individual DMM and EC/OC data are not always consistent in their trends for the lower-ethanol blends, reflective of the difficulties in measuring PM at the ~1 mg/mi level. Particle number measurements show a similar circa 20% improvement from E0 to E17 fuel. But even with somewhat lower variability than the PM mass data, this ~20% falls within the overall measurement uncertainty.

Figure 4 shows that engine-out HC and NO_x emissions exhibit similar dependences on fuel ethanol content. The decreases are more modest, about 20%. For calibration A, they occur already for the E17 blend, but calibration B data in Figure S4 indicate the decreases to occur above E17. The HC decrease

should be interpreted with caution. Adding ethanol to gasoline changes HC composition, increasing the proportion of alcohols and aldehydes. These compounds are less efficiently detected by FID, which by itself can lead to an apparent emissions reduction. Additional measurements to correct under-determination of these compounds were not conducted in this study.

PM Mode and Size

Engine exhaust particles have an agglomerate morphology; thus, their size is characterized by the notion of an equivalent diameter. The DMM employs a combination of mobility and aerodynamic analysis, but does not directly measure either equivalent diameter. Rather, we derive estimates of geometric mean mobility diameter by assuming a bimodal lognormal distribution of particle number concentration versus mobility diameter and fitting the DMM impactor and mobility currents to the calculated currents. This is similar to the procedure described previously for the ELPI (Maricq et al. 2006). The number of adjustable parameters is reduced to three by fixing the nucleation mode geometric mean diameter to 20 nm, its standard deviation to 1.3, and by assigning the universal value of 1.8 to the accumulation mode geometric standard deviation (Harris and Maricq 2001). Best fits of the DMM data and a typical OC density of 0.8 g/cm^3 yield nucleation mode masses increasing from 2% to 5% of the total PM as the ethanol content rises. Choosing a different nucleation mode diameter or standard deviation alters the calculated mass, but it remains a small fraction of the total PM mass.

The influence of ethanol level on accumulation mode diameter is illustrated in Figure 5. This shows three estimates of the geometric mean mobility diameter (μ_g): (1) ELPI, (2) fits of DMM currents, and (3) calculated from the PM mass and number measurements via:

$$M = N_0 \frac{\pi}{6} \rho_0 d_0^{(3-D_f)} \mu_g^{D_f} e^{(D_f \ln \sigma_g)^2 / 2}. \quad [1]$$

Equation (1) assumes a log-normal mobility distribution of N_0 particles with geometric mean μ_g and standard deviation σ_g, an aggregate morphology with mass-mobility exponent $D_f = 2.3$, a primary particle density of $\rho_0 = 2$ g/cm^3, and a primary particle diameter of $d_0 = 20$ nm typical of engine soot (Maricq et al. 2006). Fits of DMM data yield mean mobility diameters of ~150 nm, roughly double the size normally expected for combustion engines. This discrepancy is systematic but independent of the agreement between DMM and filter-based PM mass values. Figures 3 and S3 show that PM mass measurements from the two DMMs, ELPI, and EC/OC agree within the test-to-test variability. The question of size is discussed further in the Supplementary Information. Here, scaling the DMM values by 0.5 provides a consistent estimate of mean mobility equivalent particle diameter. The results reveal that accumulation mode particle diameter is essentially independent of ethanol level. For the E0–E17 fuels, average size may decrease a bit (~5 nm)
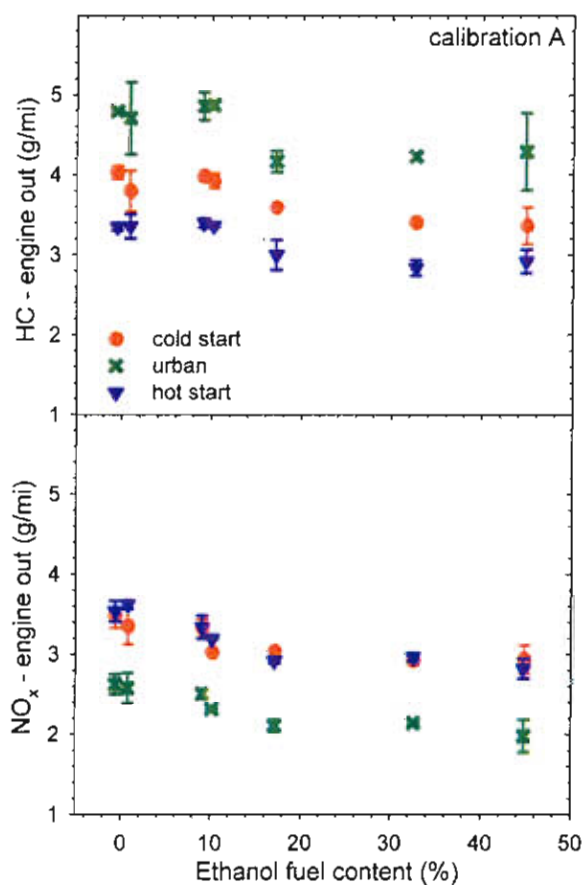

FIG. 4.   FTP engine-out (feedgas) total hydrocarbon and NO_x emissions versus fuel ethanol content for calibration A. Initial and final E0 tests are distinguished as in Figure 3. (Color figure available online).
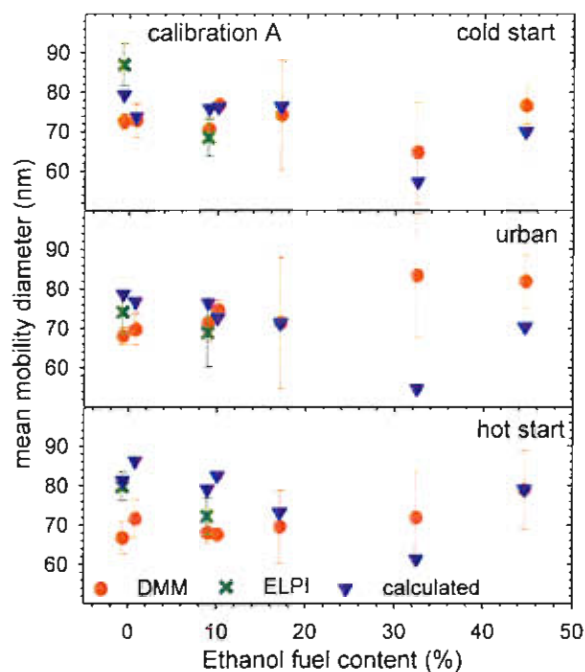
FIG. 5. Geometric mean mobility diameter of GDI particle emissions versus fuel ethanol. (Color figure available online).

from cold start to warmed-up operation and from calibration A to calibration B (Figure S5). For E32 and E45, such changes are within measurement uncertainty.

EC/OC Composition

Figures 6 and S6 plot the elemental and organic carbon fractions of the PM emissions versus ethanol blend. EC is clearly the predominant component and follows the same trend as total PM mass, namely it decreases slightly from 0% to 17% ethanol, but falls by ~45% for E32 and E45. In contrast, the OC component increases from about 0.1 mg/mi to 0.4 mg/mi from E0 to E45.

The low OC fraction is consistent with the small (<5%) nucleation mode mass determined from DMM data. However, this result should not be interpreted too literally. First, pyrolysis during thermal evolution of the OC introduces a bias toward a higher EC/OC ratio. Second, the ~0.5-mg/mi correction for gaseous HC adsorption by quartz filters is only approximate. Nevertheless, OC constitutes a small fraction of the GDI vehicle PM emissions.

DISCUSSION

Overall, the effects of ethanol blends on GDI vehicle PM emissions described above agree with previous work. The data in Storey et al. (2010) show a 30% PM decrease for E20, but as for the present study, this decrease lies within measurement uncertainty. In He et al. (2010), there is likewise no clear distinction between E0 and E10, but they report a statistically significant 20% PM reduction for E20. Interestingly, He et al.
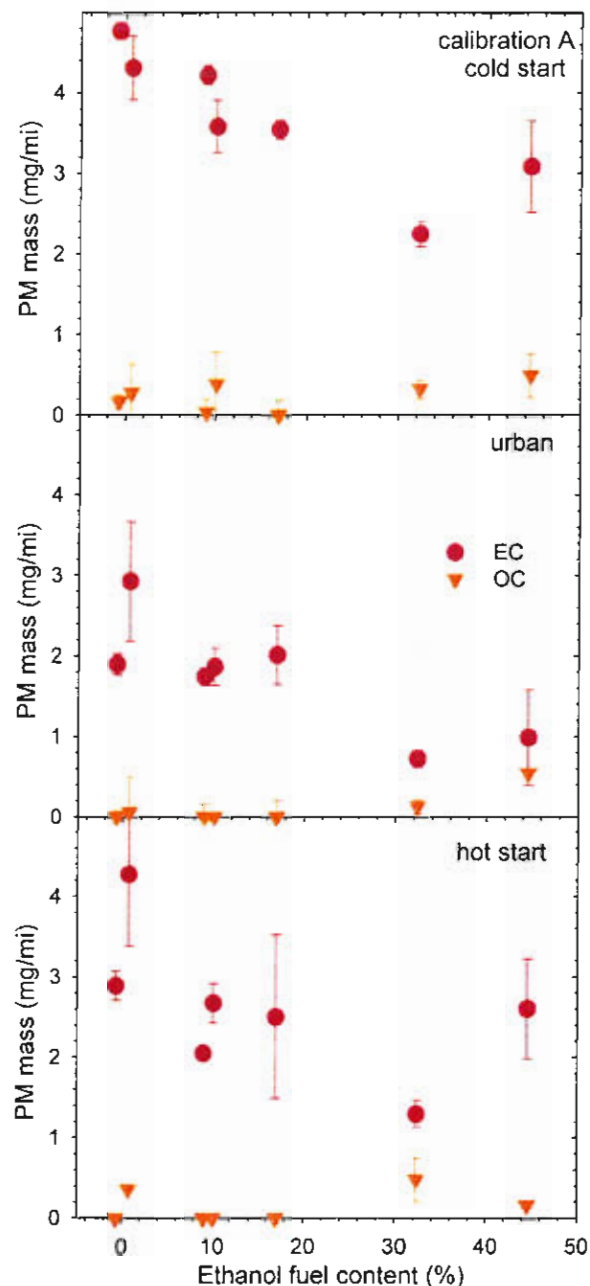

FIG. 6. Elemental carbon/organic carbon PM emissions versus fuel ethanol. (Color figure available online).

(2010) observe bimodal size distributions in their fast mobility particle sizer data, with peaks at 10 nm and 70 nm. The latter value coincides with the ~70-nm mean accumulation mode mobility diameter depicted in Figure 5. They further report that a three-way catalyst reduces nucleation mode emissions, consistent with the present DMM data, which indicate that this mode contributes little to the total PM mass from the three-way catalyst-equipped test vehicle.

The present study of GDI vehicle exhaust PM reveals interesting features not typically associated with gasoline vehicles:

582   M.M. MARICQ ET AL.
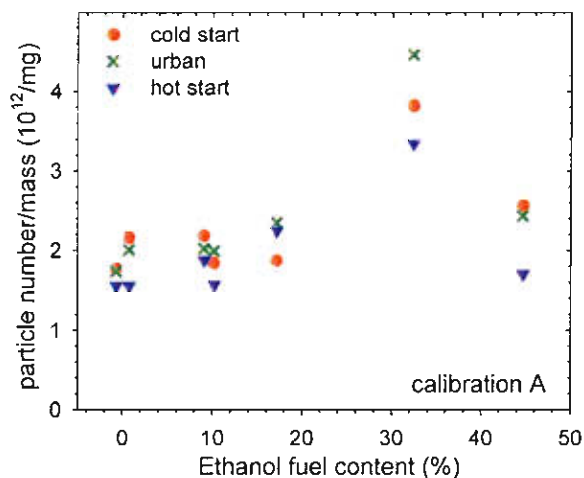

FIG. 7. Particle number to PM mass ratio versus fuel ethanol. (Color figure available online).

(1) a high fraction of elemental carbon and (2) a correlation between particle mass and number emissions. Normally, gasoline vehicle PM is considered primarily organic in nature; for example, EPA's Kansas City Study reports that OC accounts for about 80% of the particulate emissions (U.S. Environmental Protection Agency 2008). The explanation is that tight control of air/fuel stoichiometry allows little chance for sooting conditions to develop and, therefore, the observed PM largely derives from organic combustion byproducts and fugitive low-volatility fuel and lube components. But this reasoning applies to port fuel injection, where the fuel is vaporized at the intake port. Direct injection provides less opportunity for fuel vaporization and increases the likelihood of fuel impingement onto piston and cylinder surfaces, and the resulting combustion of liquid fuel produces soot. HC precursors to organic PM, though, are removed by the three-way catalyst, leaving the tailpipe PM with a high EC/OC content.

Figures 7 and 7S demonstrate the correlation between particle number and mass emissions. The ratio of $\sim 2 \times 10^{12}$ particles/mg for E0–E17 fuels is the same as found for solid particles emissions from both GDI and diesel vehicles (Kirchner et al. 2010; Maricq et al. 2011). Since in the present work, we did not purposefully remove liquid droplets, this similarity indicates that there is virtually no nucleation mode. Apparently, pool fires and liquid droplet combustion in GDI engines produce PM sufficiently similar to the 60- to 80-nm geometric mean mobility diameter soot in diesel exhaust to yield a comparable number to mass correlation (Harris and Maricq 2001). The increase of the ratio toward 4×10^{12} particles/mg in some tests, particularly E32, suggests the possibility of a small nucleation mode.

The high soot content and likely formation by liquid fuel combustion suggest that a comparison of GDI vehicle PM to soot in ethanol–gasoline diffusion flames may be interesting (Maricq 2011). These flames fall into two characteristic groups: (1) open flames, orange in color and emitting soot from their tips,

and (2) closed flames, yellow in color with no smoke emitted from the tip. E0 and E20 flames belong to the first group. They exhibit little difference in how soot size and number density develop with height of the flame. E50 is similar, but shows signs of reduced soot formation. In contrast, the E85 flame falls into group 2. In effect, ethanol blend combustion fundamentally follows a similar trend as found in the GDI vehicle emissions, namely a minimal impact on soot up to about E20, but then, larger reductions for high-level blends.

The present study suggests that substantial PM emissions benefits are not expected for low-level ethanol blends; at least not more than the ~ 0.7-mg/mi measurement uncertainty. But, neither is there a PM disadvantage as the commercial light-duty fuel composition moves to E10, and possibly E20. The specific conclusions from this study might change as GDI engine designs evolve, but the reproducibility of the fuel effects at two different calibrations, plus the similar behavior in flames, suggests a measure of robustness to these conclusions.

REFERENCES

Aikawa, K., Sakurai, T., and Jetter, J. J. (2010). Development of a Predictive Model for Gasoline Vehicle Particulate Matter Emissions. SAE Techical Paper No. 2010-01-2115. SAE, Warrendale, PA.

Akard, M., Oestergaard, K., Chase, R. E., Richert, J. F. O., Fukushima, H., and Adachi, M. (2004). Comparison of an Alternative Particulate Mass Measurement with Advanced Microbalance Analysis. SAE Technical Paper No. 2004-01-0589. SAE, Warrendale, PA.

California Air Resources Board. (2010). Preliminary Discussion Paper – Proposed Amendments to California's Low-Emission Vehicle Regulations – Particulate Matter Mass, Ultrafine Solid Particle Number, and Black Carbon Emissions, http://www.arb.ca.gov/msprog/levprog/leviii/meetings/051810/pm_disc_paper-v6.pdf

Chen, L., Braisher, M., Crossley, A., Stone, R., and Richardson, D. (2010). The Influence of Ethanol Blends on Particulate Matter Emissions from Gasoline Direct Injection Engines, SAE Technical Paper No. 2010-01-0793. SAE, Warrendale, PA.

Chow, J. C., Watson, J. G., Crow, D., Lowenthal, D. H., and Merrifield, T. (2001). Comparison of IMPROVE and NIOSH Carbon Measurements. Aerosol Sci. Technol., 34:23–34.

Coordinating Research Council. (2011). Reports E77-2c, Study to Determine Evaporative Emission Breakdown, Including Permeation Effects and Diurnal Emissions, Using E20 Fuels on Aging Enhanced Evaporative Emissions Certified Vehicles (2010) and E90-2a, Evaluation of Inspection and Maintenance OBD II Data to Identify Vehicles That May Be Sensitive to E10+ Blends (2011). Available at http://www.crcao.com/publications/emissions/index.html

Durbin, T. D., Miller, J. W., Younglove, T., Huai, T., and Cocker, K. (2007). Effects of Fuel Ethanol Content and Volatility on Regulated and Unregulated Exhaust Emissions for the Latest Technology Gasoline Vehicles. Environ. Sci. Technol., 41:4059–4064.

Fraser, N., Blaxill, H., Lumsden, G., and Bassett, M. (2009). Challenges for Increased Efficiency Through Gasoline Engine Downsizing. SAE Int. J. Eng., 2:991–1008.

Giechaskiel, B., Dilara, P., Sandbach, E., and Andersson, J. (2008). Particle Measurement Programme (PMP) Light-Duty Inter-Laboratory Exercise: Comparison of Different Particle Number Measurement Systems. Meas. Sci. Technol., 19:095401.

Harris, S. J., and Maricq, M. M. (2001). Signature Size Distributions for Diesel and Gasoline Engine Exhaust Particulate Matter. J. Aerosol Sci., 32:749–764.

He, X., Ireland, J. C., Zigler, B. T., Ratcliff, M. A., Knoll, K. E., Alleman, T. L., et al. (2010). The Impacts of Mid-Level Biofuel Content in Gasoline on SIDI Engine-Out and Tailpipe Particulate Matter Emissions. SAE Technical Paper No. 2010-01-2125. SAE, Warrendale, PA.

Kar, K., and Cheng, W. K. (2009). Speciated Engine-Out Organic Gas Emissions from a PFI-SI Engine Operating on Ethanol/Gasoline Mixtures. SAE Technical Paper No. 2009-01-2673. SAE, Warrendale, PA.

Keskinen, J., Pietarinen, K., and Lehtimäki, M. (1992). Electrical Low Pressure Impactor. *J. Aerosol Sci.*, 23:353–360.

Khalek, I. A., Bougher, T., and Jetter, J. J. (2010). Particle Emissions from a 2009 Gasoline Direct Injection Engine Using Different Commercially Available Fuels. SAE Technical Paper No. 2010-01-2117. SAE, Warrendale, PA.

Kirchner, U., Vogt, R., and Maricq, M. (2010). Investigation of EURO-5/6 Level Particle Number Emissions of European Diesel Light Duty Vehicles. SAE Technical Paper No. 2010-01-0789. SAE, Warrendale, PA.

Knoll, K., West, B., Huff, S., Thomas, J., Orban, J., and Cooper, C. (2009). Effects of Mid-Level Ethanol Blends on Conventional Vehicle Emissions. SAE Technical Paper No. 2009-01-2723. SAE, Warrendale, PA.

Mamakos, A., Ntziachristos, L., and Samaras, Z. (2006). Evaluation of the Dekati Mass Monitor for the Measurement of Exhaust Particle Mass Emissions. *Environ. Sci. Technol.*, 40:4739–4745.

Maricq, M. M. (2011). Soot Formation in Ethanol/Gasoline Fuel Blend Diffusion Flames. *Combust. Flame*, 159:170–180.

Maricq, M. M., Podsiadlik, D. H., and Chase, R. E. (1999). Examination of the Size-Resolved and Transient Nature of Motor Vehicle Particle Emissions. *Environ. Sci. Technol.*, 33:1618–1626.

Maricq, M. M., Szente, J., Loos, M., and Vogt, R. (2011). Motor Vehicle PM Emissions Measurement at LEV III Levels. *SAE Int. J. Eng.*, 4:597–609.

Maricq, M. M., Xu, N., and Chase, R. E. (2006). Measuring Particulate Mass Emissions with an Electrical Low Pressure Impactor. *Aerosol Sci. Technol.*, 40:68–79.

Ntziachristos, L., and Samaras, Z. (2010). The Potential of a Partial-Flow Constant Dilution Ratio Sampling System as a Candidate for Vehicle Exhaust Aerosol Measurements. *J. Air Waste Manage. Assoc.*, 60: 1223–1236.

Storey, J. M., Barone, T., Norman, K., and Lewis, S. (2010). Ethanol Blend Effects on Direct Injection Spark-Ignition Gasoline Vehicle Particulate Matter Emissions. SAE Technical Paper No. 2010-01-2129. SAE, Warrendale, PA.

U. S. Energy Information Administration (2011). Petroleum & Other Liquids: Weekly Supply Estimates. Available at http://www.eia.doe.gov/dnav/pet/pet_sum_sndw_dcus_nus_w.htm

U. S. Environmental Protection Agency (2007). Renewable Fuel Standard. Available at http://www.epa.gov/otaq/fuels/renewablefuels/index.htm

U. S. Environmental Protection Agency (2008). Analysis of Particulate Matter Emissions from Light-Duty Gasoline Vehicles in Kansas City. Available at http://www.epa.gov/oms/emission-factors-research/420r08010.pdf

U. S. Environmental Protection Agency (2010). EPA Announces E15 Partial Waiver Decision and Fuel Pump Labeling Proposal. Available at http://www.epa.gov/otaq/regs/fuels/additive/e15/420f10054.htm

Yi, J., Wooldridge, S., Coulson, G., Hilditch, J., Iyer, C. O., Moilanen, P., et al. (2009). Development and Optimization of the Ford 3.5L V6 EcoBoost Combustion System, *SAE Int. J. Eng.*, 2:1388–1407.